University College of Southeast Norway

www.usn.no

FMH606 Master's Thesis 2017

Process Technology

# Study of $CO_2$ storage in oil reservoirs and aquifers

Loredana Gjerden

Faculty of Technology, Natural sciences and Maritime Sciences

Campus Porsgrunn

University College of Southeast Norway

www.usn.no

FMH606 Master's Thesis, course code FMH606

**Title**: Study of $CO_2$ storage in oil reservoirs and aquifers

**Number of pages**: 56 + Appendices

**Keywords**: $CO_2$ - EOR, $CO_2$ – Storage, Oil reservoirs and aquifers


| | |
|---|---|
| **Student:** | Loredana Gjerden |
| **Supervisor:** | Britt M.E Moldestad, Nora C.I Furuvik |
| **External partner:** | InflowControl AS, Haavard Aakre |
| **Availability:** | Open |


**Approved for archiving:** _____

(supervisor signature)


**Summary:**

Carbon dioxide storage in oil reservoirs and aquifers is one of the most promising research fields regarding reduction of climate gas emissions. Changing of $CO_2$ physical properties with temperature and pressure in deep aquifers allows a great storage potential, especially in reservoir formations with high porosity and secure cap rock such as in Utsira Formation. Geological monitoring of this reservoir uncovered a theoretical potential storage capacity for about 600 Mt of $CO_2$ by producing formation water from the reservoir.

Production of formation water followed by extraction of already injected $CO_2$ in reservoir may cause great economical disadvantages and weaken the storage process. This work studies the results of simulation cases where inflow control devices, ICD and AICV valves, modeled in different arrangements and permeability zones along the wellbore, may offer a better alternative to minimize and maybe avoid $CO_2$ extraction from the reservoir. A potential advantage of using these valves in order to increase water production and decrease gas extraction is evaluated from an economic point of view. Replacing the accumulated water from the reservoir, without significant amount of bi-produced $CO_2$, could assure a great potential of CO2 storage. The exploiting time of these valve arrangements is a very important. The gas breakthrough increases production costs at the surface because of the separation and reinjection of extracted $CO_2$. This may require further experiments with different valve allocations in permeability zones and with different functional configurations.



*The University College of Southeast Norway takes no responsibility for the results and conclusions in this student report.*

# Preface

This Master Thesis is a result of a research work carried out in spring 2017 at Telemark University College, Faculty of Technology, Porsgrunn.

$CO_2$ storage in oil reservoirs and aquifers is a large research area still to explore and analyze in future. Great work on this subject is already began with Sleipner project in North Sea. Geological and experimental data on $CO_2$ storage potential of oil reservoirs and aquifers are still to be find and analyzed. The storage process has to assure a $CO_2$ capture for many thousands of years.

I would like to express my sincerely appreciation to my supervisors Britt Margrethe Emilie Moldestad and Nora Cecilie Ivarsdsatter Furuvik for their great help all the way through this work.
They have guided and encouraged me with their knowledge and patience to work on this subject.

Porsgrunn, May 11, 2017

Loredana Gjerden

# Nomenclature

| Abbreviation | Description | Unit |
|---|---|---|
| a | reservoir area | [$m^2$] |
| **AICV** | Autonomous Inflow Control Valve | [-] |
| **ICD** | Inflow Control Device | [-] |
| **cP** | Centipoise, (1 cP = 1 m Pa·s) | [-] |
| **CCS** | Carbon Capture and Storage | [-] |
| **D** | Darcy, Unit for Permeability | [mD] |
| **Drn** | Drainage | [-] |
| **EOR** | Enhanced Oil Recovery | [-] |
| **Imb** | Imbibition | [-] |
| **k** | Permeability | [mD] |
| **k*g*** | Effective permeability to gas phase | [mD] |
| **k*o*** | Effective permeability to oil phase | [mD] |
| **k*ro*** | Relative permeability to oil phase | [-] |
| $\mathbf{k_{rgcw}}$ | Relative permeability to oil at irreducible water saturation | [-] |
| $\boldsymbol{k_{rwgc}}$ | Relative permeability to water at residual oil saturation | [-] |
| k***rw*** | Relative permeability to water phase | [-] |
| k***w*** | Effective permeability to water phase | [mD] |
| m | Mass | [kg] |
| $\boldsymbol{n_w}$ | Corey coefficient for water | [-] |

| | | |
|---|---|---|
| $k^{i}_{rw}$ | Water relative permeability for imbibition | [-] |
| $k^{d}_{rw}$ | Water relative permeability for drainage | [-] |
| $k^{i}_{rg}$ | Gas relative permeability for imbibition | [-] |
| $k^{d}_{rg}$ | Gas relative permeability for drainage | [-] |
| $k^{r}_{CO2}$ | Endpoint $CO_2$ relative permeability | [-] |
| $n_g$ | Corey coefficient of gas | [-] |
| $S$ | Saturation | [fraction] |
| $S_{gc}$ | Gas saturation | [fraction] |
| $S_{or}$ | Residual oil saturation | [fraction] |
| $S_w$ | Water saturation | [fraction] |
| $S_{rw}$ | Residual water saturation | [fraction] |
| $S_{max}$ | Endpoint saturation | [fraction] |
| $S_t$ | Residual or trapped saturation | [fraction] |
| $S_{iw}$ | Irreducible water saturation | [fraction] |
| $Sm^3$ | Standard cubic meter (cubic meter at t =15℃ and p=1,01325 bar) | [-] |
| V | Volume | [$m^3$] |
| $p_{CO2\_res}$ | $CO_2$ pressure at reservoir conditions | [bar] |
| $p_{CO2\_surf}$ | $CO_2$ pressure at surface conditions | [bar] |
| $V_{CO2\_res}$ | $CO_2$ volume at reservoir conditions | [$m^3$] |

| | | |
|---|---|---|
| $V_{CO2\_surf}$ | $CO_2$ volume at surface conditions | [$m^3$] |
| $T_{CO2\_res}$ | $CO_2$ temperature at reservoir conditions | [K] |
| $T_{CO2\_surf}$ | $CO_2$ temperature at surface conditions | [K] |
| E | Storage efficiency factor | [%] |
| N/G | Net-to-Gross ratio | [-] |
| h | gross reservoir thickness | [m] |

| Greek letters | Description | Unit |
|---|---|---|
| **Φ** | Effective porosity | [fraction] |
| ρ | Density | [kg/m$^3$] |
| θ | Contact angle | [degrees] |

# List of figures

# List of tables

# Contents

# 1. Introduction

The storage of captured $CO_2$ in deep saline aquifers is of the greatest importance regarding the global warming along with climate changing and pollution.
The Utsira Formation is geologically described as porous and permeable reservoir, mostly sandy especially at the Utsira Sand and with a considerable good depth for storing fluid $CO_2$ (700 to 3000 meters).

Sleipner is the leading project that works on carbon capture and storage under the sea level since 1996. The $CO_2$ injection and storage has achieved great results in long terms at the Sleipner field. The injection capacity has been about 1Mt $CO_2$ per year since 1996 and the storage potential has been improved since.

The excellent storage capacity and the high permeability predict a great possibility to store even more carbon dioxide by extracting the formation water from the aquifer and deposit it in to the ocean.
It is estimated that a complete extraction of the formation water from the Utsira and the replacement of it with $CO_2$ may assure a theoretical storage capacity of 600 Mt $CO_2$.

The purpose in this study is to evaluate the capability to store $CO_2$ in offshore saline aquifers with characteristics close to Utsira Formation by replacing the volume of extracted reservoir water with $CO_2$ in order to ensure long-term storage. Physical properties of carbon dioxide, as an injection gas utilized to enhance oil recovery and for storage purposes in deep saline aquifers, are described in Chapter 2. The reservoir properties and the potential to store $CO_2$ are in order to calculate the storage capacity in Chapter 3. The correlations between reservoir properties experimental data are considered in the simulations carried out using ROCX-OLGA. The simulation models are described in Chapter 4. The methods used to estimate a possible solution are presented in these chapters.

The quality of the extracted water is not an issue here, but the amount of extracted gas along with the produced water may cause a deficit to the $CO_2$ storage project. This is no longer a successful storage process when the separation of the gas from water implies high expenses at the surface.

Extracting water and gas from the reservoir can be evaluated as non-economical if the process continues to produce gas even in a minor scale over a large time scale.

There are possible advantages when using one or several methods discussed in chapter 5.
Criteria such as accumulated water amount in short time before the gas breakthrough, the accumulated water amount over a longer period, when extracted amount of gas increases more or less, are taken into account. An economic overview may clarify which alternative is most profitable.
Using internal control devices, the water extraction can be controlled and the gas breakthrough from offending zones can be reduced or even shot off. The variety of permeabilities in the reservoir depends on the wettability of soil. The operating principles of the control valves can optimize the well design and water production with respect to porosity thickness along the wellbore.
The characteristics of the control devices and their displacement along the pipe implicate the capacity to respond to and control, as quickly as possible, the gas flow into the pipe by slowing down the inflow or even temporary close the water extraction process. [1], [25], [27], [28]

# 2. Carbon dioxide for enhanced oil recovery and storage in aquifers

The reduction of carbon dioxide in atmosphere by storing the gas underground is one of the most important actions to reduce the pollution and its influence over the climate changes.
The green house effects on climate are increasing with increasing concentration of $CO_2$ in the atmosphere. The International Energy Agency estimates that the global emissions of $CO_2$ increase to about 57 $GtCO_2$ per year.
Capture and storage (CCS) of "man-made" $CO_2$ emissions relies on better storage technologies and more cost effective processes to ensure a long-term deposit of carbon dioxide. [32]

## 2.1 Carbon dioxide as injection gas for EOR

Carbon dioxide injection for oil recovery (EOR) is one of the most known and economically rational method to enhance oil production and to sequestrate $CO_2$ in a reservoir.

The changing of $CO_2$ properties at the reservoir pressure and temperature makes the oil more mobile and easier to displace from the reservoir pores. [8]
Transport and injection of $CO_2$ happens in the supercritical phase, as shown in
Figure 2-1.

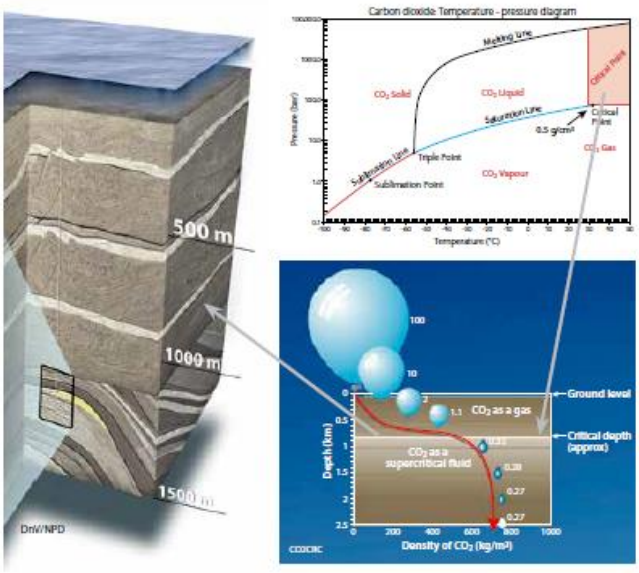


Figure 2-1 $CO_2$ behavior at different temperature, pressures and depth [34]

$CO_2$ injection in offshore saline aquifers gives a long term assurance because these can store large volumes of $CO_2$ far away from land avoiding gas leakage risks. They have thick successions of tight clay or shale cap-rock and are often associated with petroleum exploration and production with infrastructure capable of $CO_2$ storage development. [31]

## 2.2 $CO_2$ storage in aquifers

An aquifer is a defined as a porous and permeable sedimentary rock where the water in the pores may consist of several sedimentary formations and cover large areas.

The capture and storage of carbon dioxide in deep saline aquifers is most preferable because of their geological storage qualities such as tight clay or shale cap-rocks. The saline aquifers present also storage advantages due to the information from petroleum explorations and production.

The cap-rock gather the stored $CO_2$ above the close underlaying aquifer in this way closing for a possible migration of the gas upward.

The Utsira Skade aquifer is one of ten aquifers that was evaluated as suitable for $CO_2$ storage in the northern North Sea because it has porous and permeable sands, ideal depth levels for storing $CO_2$ and good seals. They can store gigatonnes of $CO_2$.

Once deposited in the saline aquifer, the gas migrates through the interconnected pore spaces in the rock and forms a gas cap, see Figure 2-2.

In order to limit the reservoir pressure that assures the $CO_2$ injection and storing, sufficiently water has to be produced from the reservoir.

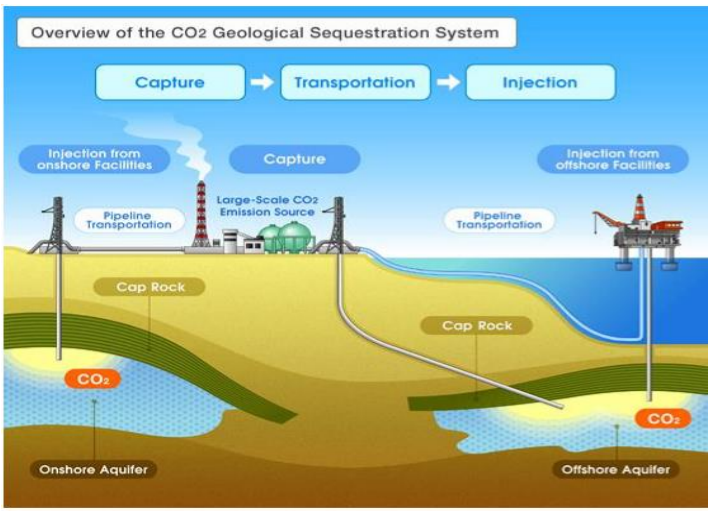


Figure 2-2 Geological storage of $CO_2$ [32]

This advantageous geological structure opened for the largest capture and storage program conducted by the Sleipner-project in Norway. The injection time for pure CCS in the Utsira Sand, Norwegian sector, were about 1Mt $CO_2$/year at 800m depth since 1996.

Several research describe the Sleipner operations as a leading performer within injection and storage of $CO_2$ at Utsira. [3], [5], [28]

The saline aquifers have a great potential $CO_2$ storage because of their size, porosity and permeability and the depth under the sea level. The size of the reservoir must be large enough to store the demanded of $CO_2$ quantities for one power plant with lifetime emissions.The porosity and permeability must assure sufficient pore volume for injection and storage of $CO_2$. The physical properties of $CO_2$ at high pressure and temperatures, determined by the depth under the sea level, allows great volumes of stored $CO_2$.

Figure 2-3 shows that the critical temperature of $CO_2$ is about 31C° and the density changes dramatically with the temperature and pressure.

At the reservoir conditions such as the conditions used in this work (100 °C and 130 bar), carbon dioxide is in supercritical phase and has a density of 274, 76 kg/$m^3$.

Research on $CO_2$ storage offshore shows that $CO_2$ should be in supercritical or liquid state during transport and injection.

Density of carbon dioxide is strongly dependent of pressure, temperature and depth. At 700-800 meters below the sea level, $CO_2$ is in supercritical phase, which advantageously can be stored in the Utsira Formation.

The density of $CO_2$, $\rho_{CO2}$, increases with pressure but decreases with temperature. As a function of depth, the density increases monotonically as the pressure effect also overcompensates the temperature effect.

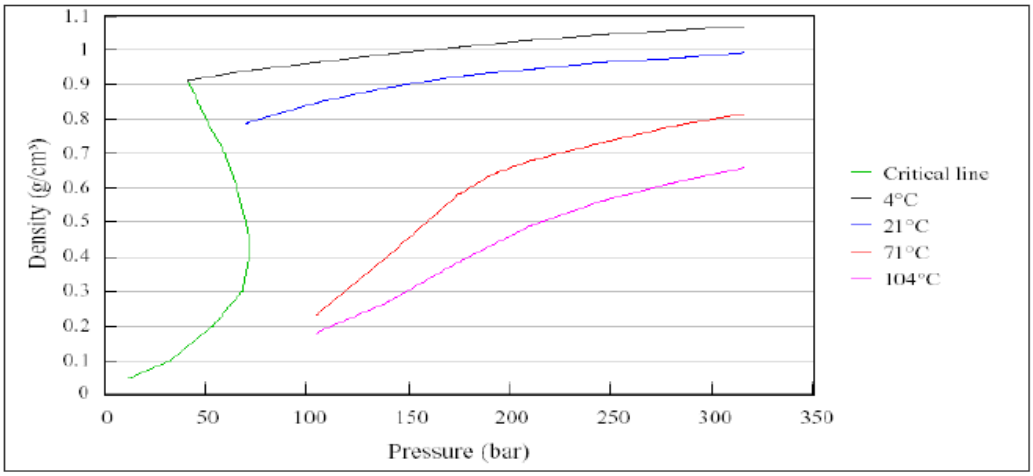


Figure 2-3 $CO_2$ density depending on temperature and pressure [33]

The black curve in Figure 2-3 shows that the $CO_2$ density increases more with increasing pressure at temperatures above the critical point but the curve slope for higher temperature than 70°C is steeper with increasing pressure from about 100 bar to 200 bar.

At the reservoir temperature assumed as 100°C and a pressure assumed as 130 bar, the density of $CO_2$ may be readed from purple curve as around 0.27 g/cm$^3$.

The dissolution of injected $CO_2$ into the reservoir water makes the mixed fluid to sink towards the bottom of the reservoir. The simulations described further in this work are influenced by the increased concentration of $CO_2$ of the pore fluid and the permeability of the zones along the wellbore.

Data from Sleipner field estimates that 15% of injected $CO_2$ will dissolve in reservoir water after 10 years. [6], [20], [26]

# 3. $CO_2$ storage capacity in Utsira formation

Utsira formation is the largest aquifer - about 2.6 x $10^4$ $km^2$ - in the North Sea and has been topographically described as one of the most suitable storage reservoir. With an estimated pore volume of 5.5 x $10^{11}$ $m^3$, the theoretical $CO_2$ storage potential may become as large as 600 Gt if the complete exchange of the formation water with $CO_2$ is possible.

The extraction of the formation water contains variable amount of $CO_2$ depending on the wettability of the reservoir. The challenge is then to avoid the production of already stored $CO_2$ as much as possible.

The water production from a reservoir with great storage capacity and the water replacement potential is not depending only of wettability but is dependent of porosity and permeability of the reservoir as well.

During the drainage process, the formation water is extracted from the rock pore and the $CO_2$ will occupy the available pore space as shown in Figure 3-1.

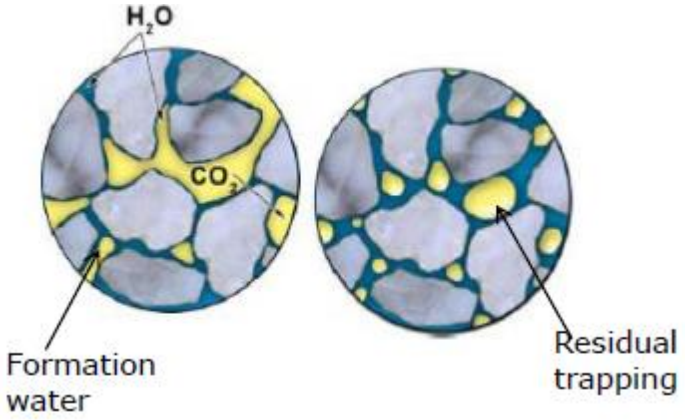


Figure 3-1 Trapping of $CO_2$ by the formation water [9]

By replacing the water in pores with $CO_2$, some of $CO_2$ will dissolve and some of $CO_2$ will be captured in smaller pores. This is called residual trapping. The viscosity of $CO_2$ at high temperatures and pressures is still lower (about 0.0252 cP) than viscosity of water at the same conditions (about 0.285 cP). This makes $CO_2$ to flow easier as a continuous flow in between the reservoir pores and further to the wellbore.

The capacity of $CO_2$ storage is strongly dependent of pressure, temperature, and the geological structure of the reservoir that must assure the supercritical or liquid $CO_2$ phase. Other important dependences are the cap rock sealing effectiveness with limited vertical flow. These conditions at Utsira have been estimated as suitable for $CO_2$ storage below 700-800m under the sea ground. [11], [28], [33], [35]

## 3.1 Utsira reservoir properties

The Sleipner $CO_2$ injection and storage project is located just above the Utsira Sand, see Figure 3-2. The shale drape covers this sandy reservoir and naturally assures a safe injection of $CO_2$ from the Sleipner. This cap rock makes the $CO_2$ storage secure over thousands of years. [3]

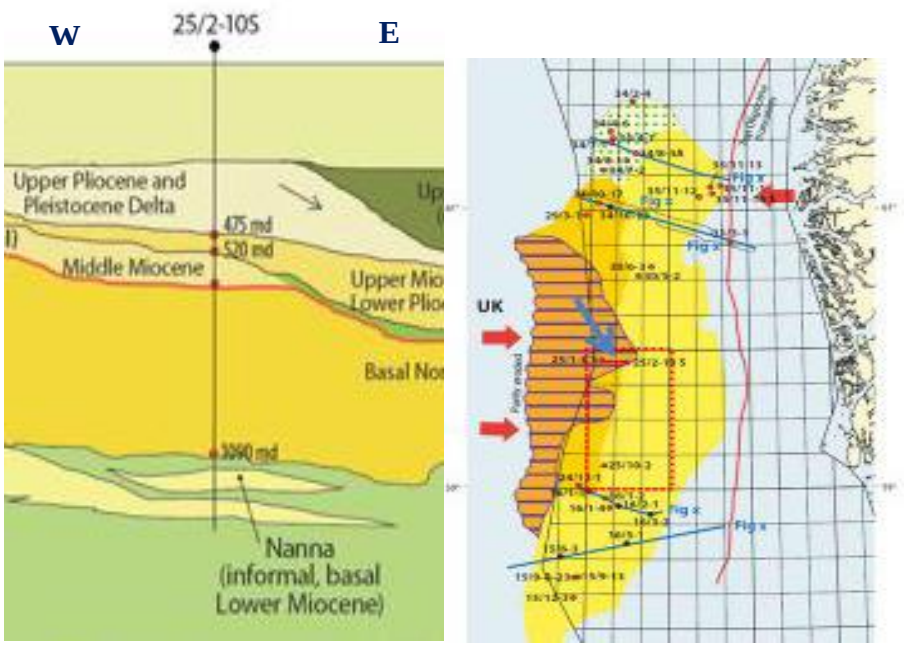


Figure 3-2 Location of Utsira formation [9]

An analysis of the topography of the top formation shows large variation in depth (Figure 3-3), and in the central western part it is actually so shallow that stored $CO_2$ may not be present in its dense phase only. It is usually assumed that $CO_2$ cannot effectively be stored at depths above 700 m. [9], [34].

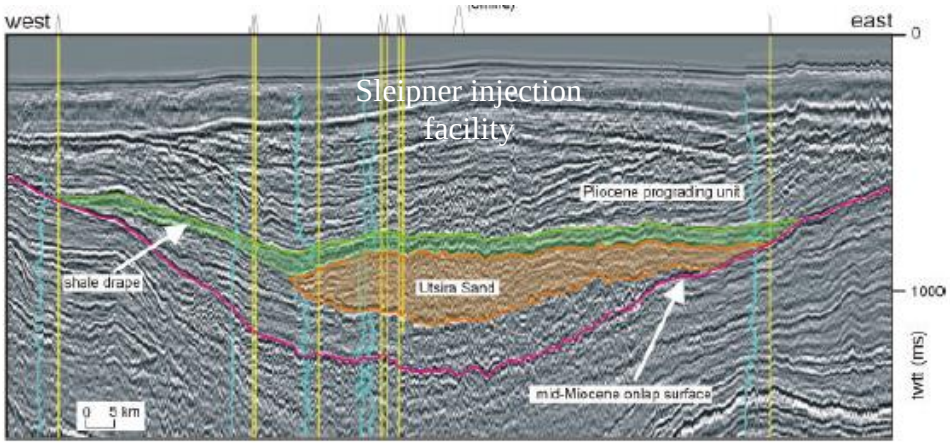


Figure 3-3 The Southern part of the Utsira Formation [3]

## 3.1.1 Wettability

Wettability describes the contact degree of a given fluid that has adhesion to a solid. If two or more fluids are present in reservoir, and these fluids are non-miscible, the most adhesive forces will describe the fluid as the wet-phase and the other as non-wet.

In the case of the Utsira Formation storage reservoir, it is presumed that the wet fluid is water and the non-wetting fluid is $CO_2$.

Figure 3-4 describes that the contact angle θ of the fluids with rock has a very important influence over fluid permeabilities between the rock pores. If the fluid–rock contact angle is < 90° then that fluid preferentially covers the pore surface and it becomes known as the 'wetting fluid'. Under typical reservoir conditions, the water will be the wet-phase and injected $CO_2$, with a contact angle of >90◦, will be the non-wetting phase.

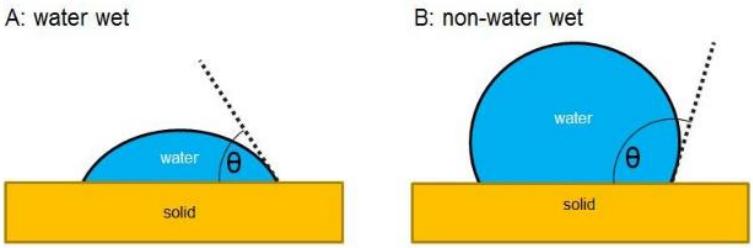


Figure 3-4 Contact angle θ for A) water-wet reservoir and B) non water-wet reservoir [30]

Wettability influence the gas or oil flow, during the water extraction. In a water-wet reservoir, the gas is more mobile than water, as shown in Figure 3-5.

Some of injected $CO_2$ will imbibe the available pore space; some of it will dissolve in the water and sink in the reservoir.

Depending on the reservoir pore size and entrance pressure of $CO_2$ in these pores, $CO_2$ saturation increases. This results in a waterfront that force both gas and water toward wellbore. When the $CO_2$ pressure is insufficient to replace water in small pores, water will remain in place. This is the lowest water saturation in situ when gas flows through a water saturated reservoir rock. This can be seen in Figure 3-5.

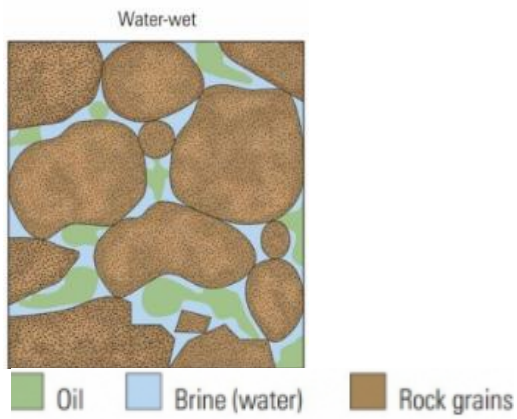


Figure 3-5 Wettability in pores for a water-wet reservoir [29]

In a porous medium consisting of rock, oil and water system will be water-wet when water occupies the smallest pores and in contact with the surface of the rock in the largest pores. [29], [30]

## 3.1.2 Porosity and permeability in aquifers

Porosity of a reservoir is the ratio between the total pore volume (the "void space" between the grains) and the total volume of the reservoir (bulk volume). Porosity describes the ability of the reservoir to store fluids:

$$\phi = \frac{\text{pore volume}}{\text{bulk volume}} = \frac{\text{bulk volume} - \text{grain volume}}{\text{bulk volume}} \qquad [3\text{-}1]$$

Data from the Sleipner area suggest that the porosity of the Utsira Sand is high. Microscopic modal analysis of thin sections gives porosities generally in the range 27% to 30%; geophysical log porosities are slightly higher, between 30 and 40%. [20], [25]

A high porous rock allows the reservoir fluids to flow through these pores by a network of interconnections. This network is called permeability. A reservoir is high permeable when the fluid transport is high and less permeable or impermeable when the transport of fluid is small or almost impossible, see Figure 3-6.

The $CO_2$ flow through the interstitial channels depends on capillary pressure between the pores and the pore size. The affinity of water to the sand grains, such as in a water-wet reservoir, and the viscosity difference between water and carbon dioxide traps rests of water in between microscopic channels. The trapped water has then what it is called residual saturation.

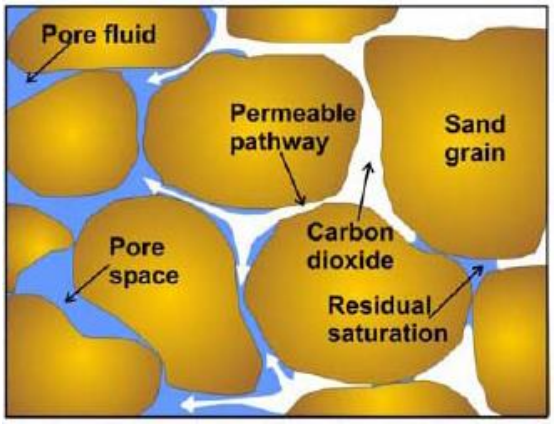


Figure 3-6 Diagram highlighting porosity and permeability [26]

## 3.1.3 Relative permeability in Utsira reservoir

As mentioned in the subchapters above, the Utsira Sand has the necessary qualities for depositing $CO_2$ over several thousands of years.

The relative permeability describes the ability of a reservoir saturated with one fluid to conduct the fluid when more than one fluid flows through the reservoir. It is dependent on the fluid saturation in reservoir, wettability and porosity. These parameters are of fundamental importance when relative permeabilities are measured.

There are many studies available about enhanced oil recovery related to relative permeability in oil fields but the amount of information for saline aquifers and gas storage capacity is not as

much comprehensive as for oil. There is still a necessity to explore and certify $CO_2$ storage capacity in the aquifers.

When $CO_2$ displaces the formation water in reservoir, the process is called drainage (the non-wetting phase takes the place of the wetting-phase).In the imbibition, the non-wetting phase permeability $CO_2$ decreases toward zero when the maximum residual saturation is reached.

The $CO_2$ endpoint relative permeability, as shown in Figure 3-7, $kr_{CO2}$ describes the relative permeability of $CO_2$ at maximum $CO_2$ saturation $S_{max}$. The $k^d_{rw}$ curve shows that the relative permeability of water sinks with increasing relative permeability of $CO_2$ under water extraction (drainage) process. [22], [36]

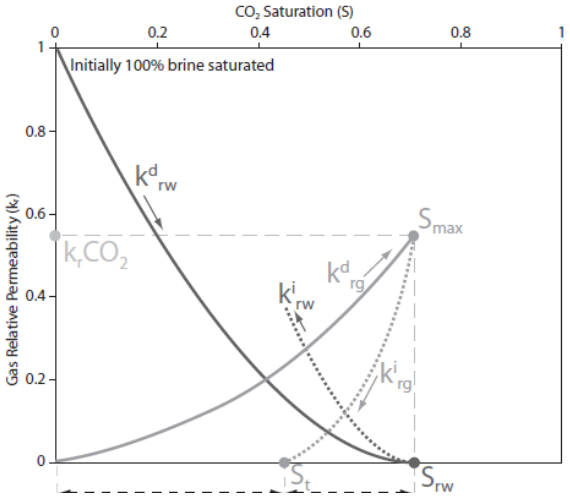


Figure 3-7 Example of a typical relative permeability curves
for drainage and imbibition recorded throughout experimentation [22]

Utsira Sand is mostly consisting of sandy, porous layers. The permeability curves from the experimental data, as shown in Figure 3-8, may characterize this part of the reservoir as water-wet with a contact angle θ between 60° and 75° and an irreducible water saturation between 20% and 25%. The simulation part in Chapter 4 use data from these experiments described in Figure 3-8. [4], [25]

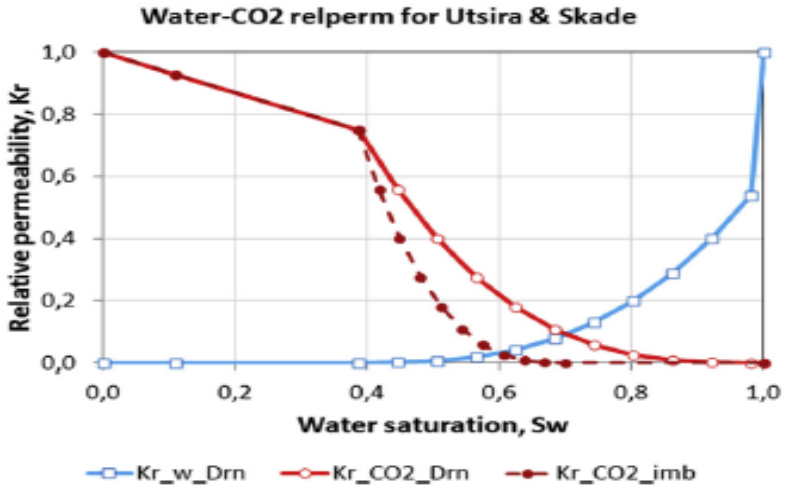


Figure 3-8 Relative permeability curves for critical $CO_2$ and water. [3]

The ROCX-data related to water saturation and oil saturation ($S_w$, respectively $S_o$) have been calculated using the generalized Corey-model developed for an wide range of rock and wettability characteristics,

$$k_{rw} = k_{rwgc}\left(\frac{S_w - S_{iw}}{1 - S_{iw}}\right)^{n_w} \quad [3\text{-}2]$$

$$k_{rg} = k_{rgcw}\left(\frac{S_g - S_{gc}}{1 - S_{gc} - S_{iw}}\right)^{n_g} \quad [3\text{-}3]$$

$S_{gc}$ is the critical gas saturation, $S_{iw}$ is the irreducible water saturation, $S_g$ and $S_w$ the gas and respectively the water saturation at reservoir conditions, $k_{rw}$ and $k_{wg}$ are the relative permeabilities to water and gas, $k_{rwgc}$ is the relative water permeability at critical gas saturation and $k_{rgcw}$ is the relative gas permeability at critical water saturation. [13], [17], [19]

The generalized Corey model describes the influence of the Corey's factors values and the relative permeabilities of the reservoir fluids.

Figure 3-9 shows the relative permeability for gas and water generated in ROCX using the Corey correlations, see Appendix B. In this figure, the red line represents the gas relative permeability and the blue curve represents the water relative permeability at Corey's factor for 2.8 for $CO_2$ respectively 8 for water.

The red curve shows that the relative permeability for $CO_{2,}$ as the imbibition fluid, increases rapidly with decreasing water saturation from a value of 0.65 to 1. The water extraction, with assumed irreducible saturation as 0.22, would permit $CO_2$ enriching of the reservoir pores at large values of gas permeability, see Figure 3-9.

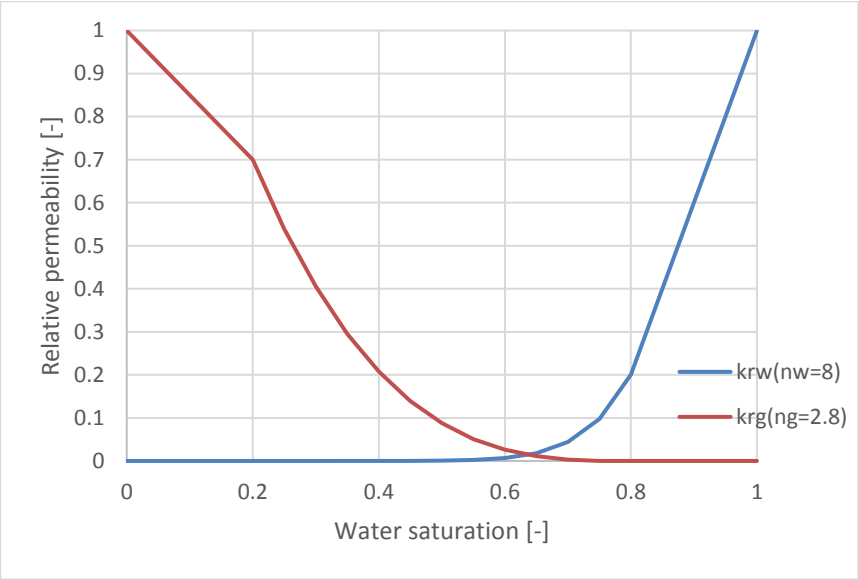


Figure 3-9 Relative permeabilities $k_{rw}$ and $k_{rg}$

The Corey's coefficients have been estimated from the experimental data that show the influence of the relative permeability for the wetting phase (water) and non-wetting phase ($CO_2$) during the water extraction and $CO_2$ reservoir enriching processes. Typical values for these factors are as shown in Table 3-1. [21], [36]

Table 3-1 Corey factor in oil-wet and water-wet reservoir [36]

| **Wetting conditions in reservoir** | **$n_o$** | **$n_w$** |
|---|---|---|
| Oil Wet | 6-8 | 2-3 |
| Water Wet | 2-4 | 6-8 |

## 3.2 Calculation of $CO_2$ storage capacity in aquifers

$CO_2$ sequestration capacity in deep saline aquifers is derived by the volumetric, top-down approach. It is based on the bulk volume of the aquifer, derived from the average available subterranean area ($m^2$) and the average thickness of the aquifers (m). This volume is then restricted to the fraction which can absorb $CO_2$, using the net-to-gross ratio.

In all reservoirs, there are zones with fluid-producing and non-producing layers as shown in Figure 3-10. The poorly porosities or permeabilities in the non-producing layers describes the degree of storage potential in these reservoirs.

The thickness of productive reservoir (net) within the total thickness (gross) of the reservoir is termed net to gross (N/G) ratio.

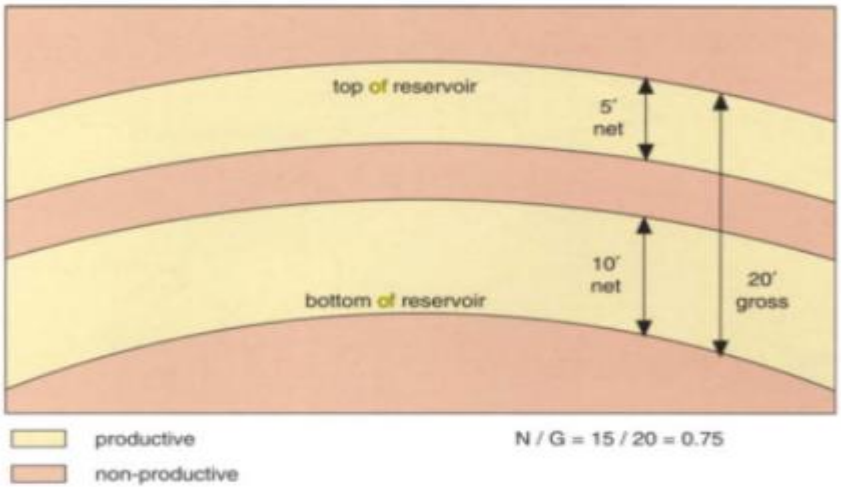


Figure 3-10 Net to gross ratio in a reservoir [37]

The net to gross ratio is not constant over the whole reservoir. It can change value over short distance between 1.0 (100% reservoir) to 0.0 (no reservoir).

In publications related to calculation methods is a consensus that the method for calculating the storage capacity of an open saline aquifer is a function of to the total pore volume in the reservoir:

$$Q = a \cdot h \cdot N / G \cdot \varphi \cdot \rho\, CO_2 \cdot E \qquad [3\text{-}4]$$

where Q = Storage capacity(Mt), a = area of the reservoir formation ($m^2$), h = gross reservoir thickness (m), N / G = mean net / gross reservoir (proportion of sediment structures with

porosity and permeability suitable for absorbing $CO_2$), φ = mean effective porosity, $\rho_{CO2}$ = density of $CO_2$ at reservoir temperature and pressure, E = storage efficiency factor.

Storage efficiency factors for rough estimates of the regional capacity of an open aquifer ranges from 1% to 6% at the minimum theoretical storage and up to 40% at the maximum storage possibility. [14], [26], [37]

Standard conditions of 1 atmosphere and 15°C change the volume accumulated at reservoir conditions to surface conditions by the gas law:

$$\frac{p_{CO2\_res} \cdot V_{CO2\_res}}{T_{CO2\_res}} = \frac{p_{CO2\_surf} \cdot V_{CO2\_surf}}{T_{CO2\_surf}} \qquad [3\text{-}5]$$

The gas density at the standard condition is 1.8475 kg/m$^3$ and at reservoir conditions 274.76 kg/m$^3$.

# 4. Simulation of water and gas extraction

The near-well simulations of formation water with $CO_2$-extraction were performed using simulation software Rocx, in combination with OLGA.

OLGA is a dynamic simulation tool for multiphase flow in pipelines with several possibilities regarding equipment, reservoir and fluid flow properties.

The simulations related to equipment uses ICD and AICV valve types. The reservoir properties, as temperature and pressure, have constant values for a more manageable overview of this study.

## 4.1 Reservoir modeling with OLGA-ROCX

The simulated reservoir in ROCX was modeled as 1000 m long, 66 m wide and 50 m high. This geometry, with respect to zones, is presented in Figure 4-1. The pipe lays 35 m from the top and 40.5m from the left. The wellbore and pipeline modeled in OLGA, is as a horizontal pipe with a length of 1000 m and a diameter of 0.1m.

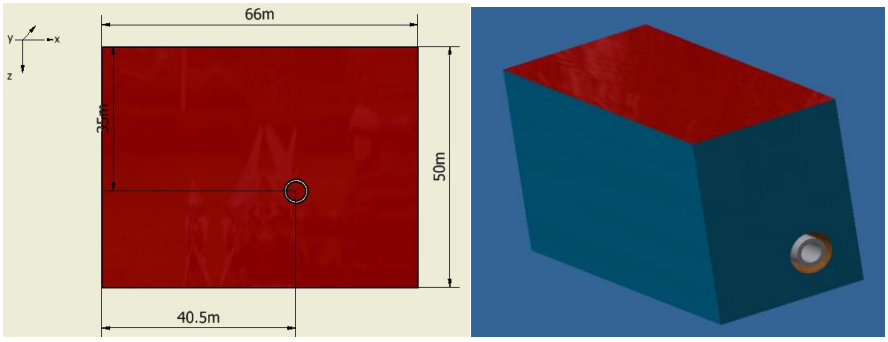


Figure 4-1 Geometry of the simulated reservoir, Autodesk Inventor

The reservoir is divided into 10 zones in x-direction, 25 in y-direction and 10 in z-direction. The each well zone is divided into two sections with source and leak into each section, see Figure 4-2 a).

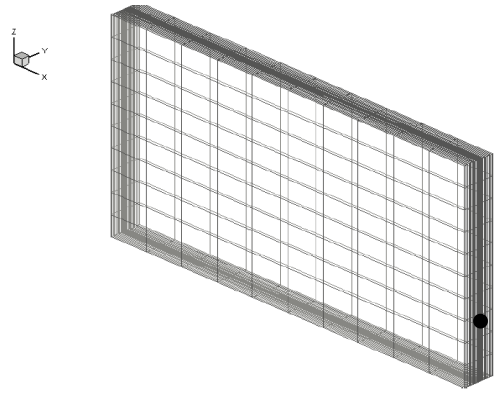

Figure 4-2 a) 3D view of the grid with the pipe location

A closer description of the modeled reservoir volume, see Figure 4-2 b, shows a front view and the section of it. The annulus and the pipe are located at the almost lowest level of the volume. This is the location used in the ROCX-simulation in order to calculate the water production in an aquifer.

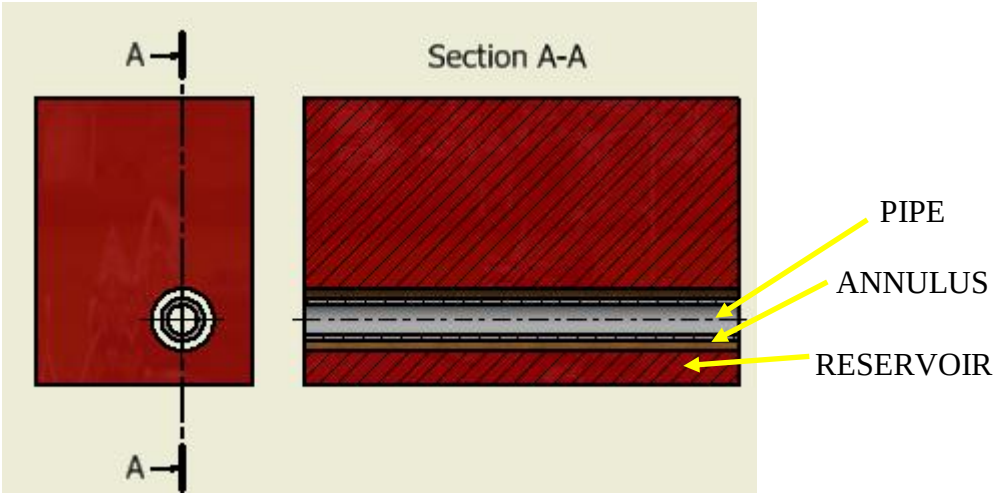


Figure 4-2 b) Section through the reservoir at the pipe position, Autodesk Inventor 2017

The permeabilities along with x-direction in these 10 sections are set to 1000 mD, 1000 mD 1000 mD, 2000 mD, 2000 mD, 2000 mD, 2000 mD, 1000 mD, 1000 mD, 1000 mD.
The *Flowpath* is divided into twenty equal sections. The *Sources* represent the flow from the reservoir to the pipeline. The sources describe the characteristics of the reservoir through ROCX-parameters.

The *Leaks* permit the water and gas inflow from the wellbore to the pipe through the ICDs or AICVs, functioning differently. The *Packers* are indicated as closed valves(Valve 1 to Valve 10) in order to isolate the wellbore sections from each other, as shown in Figure 4-3.

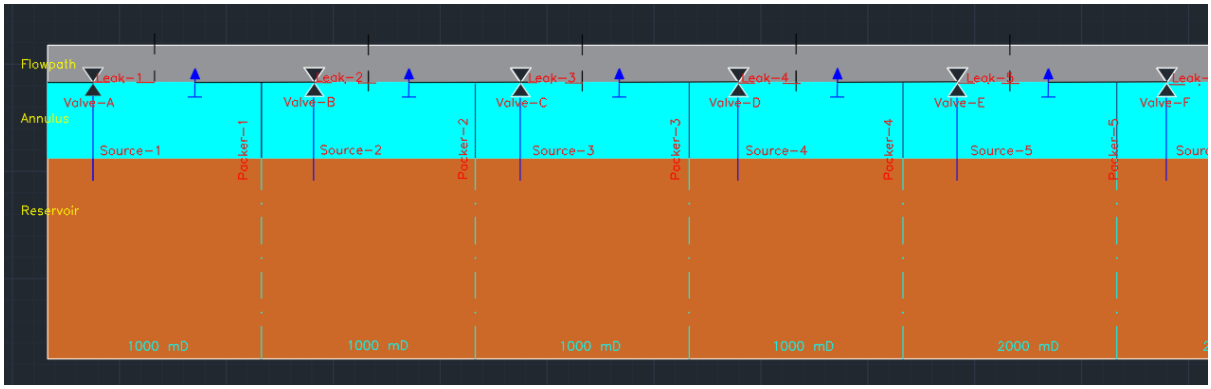


Figure 4-3 Section of near well-path showing displacement of valves, leaks and sources along with the pipe, AutoCAD 2017

The components used in the Black oil ROCX-simulation are defined as shown in Table 4-1. The water component, oil component and gas component are specified with properties related to their specific gravities, mole fraction of $CO_2$, $H_2S$ and $N_2$.

Table 4-1 Reservoir properties used in simulations

| **Oil specific gravity** | **Gas specific gravity** | **Water specific gravity** | **$CO_2$ fraction mole** | **$H_2S$ and $N_2$ fraction mole** | **Reservoir pressure (bar)** | **Reservoir temperature** | **Effective porosity assumed constant all over the reservoir** |
|---|---|---|---|---|---|---|---|
| 0.85 | 1.5 | 1 | 0.05 | $10^{-6}$ | 130 | 100 °C | 0.35 |

There are defined two feed streams: Feed 1 as $CO_2$ and Feed 2 as water. The specifications for the parameters used in ROCX for these feed streams relies on literature related to $CO_2$ storage reservoirs and water extraction processes from these reservoirs, see Table 4-2. [24]

Table 4-2 Feed streams

| **Feed/fraction type** | **Fraction** | **Watercut** |
|---|---|---|
| Feed 1_Gas/LGR | 0.001 | 0.001 |
| Feed 2_Water/GLR | 0.001 | 0.8 |

Data from ROCX are collected and processed in OLGA. This is resumed in Table 4-3.

Table 4-3 Reservoir and fluid properties used in ROCX simulations

| **Properties** | **Reservoir** | **Fluid** |
|---|---|---|
| Reservoir temperature | 100°C | 100°C |
| Reservoir pressure | 130 bar | 100 bar |
| Porosity in reservoir | 0.35 | |
| Oil specific gravity | 0.85 | |
| $CO_2$ molar fraction of gas | | 0.05 |
| Gas specific gravity | 1.5 | |
| Permeability at the the first and last 3 zones in x-y-z directions | 1000-1000-200 mD | |
| | 2000-2000-200 mD | |

The equipment shown in Figure 4-3 is described in Table 4-4. The ICD and AICV valves have the same diameter. The packers separates the zones in the wellbore in order to restrict the inflow of water and gas from neighboring zones.

Table 4-4 List of equipment list used in OLGA simulation

| **Equipment** | **Model description** | **Description** |
|---|---|---|
| ICD-valve | Diameter 0.02m sized to a pressure drop of 10 bar | CD[1] = 1<br>Connecting to the pipeline |
| AICV-valve | Controlled by PID | CD = 0.84 |
| Leak | Diameter 0.02m | CD = 1 |
| Packers | Diameter 0.1 | OLGA valve type, fully closed |

[1] CD – coefficient of discharge

## 4.2 AICV and ICD functionality in the modeled reservoir

ICD[2] and AICV[3] valves are generally used for increasing the oil production and to limit or even stop the production of water and gas from an oil reservoir. The cases simulated in this work consider possibility of using these valves to produce reservoir water and avoid as much as possible the extraction of $CO_2$ already stored in the reservoir.

The valves are placed in different permeability zones. High permeability zones may give a high production of water but a high production of gas as well. In order to assure a profitable $CO_2$ storage process, the valves can limit the gas inflow by controlling the settings in OLGA.

Figure 4-4 Nozzle type ICD, Resflow TM Schlumberger(left), AICV® inflow control device(right) [38]

There are five simulation cases based on performances of AICVs and ICDs during the process of water extraction from the reservoir, see Table 4-5.

The AICV valve has the ability to control the fluid flow into the pipe by choking for low viscosity fluid and opening for high viscosity fluid. The ICDs are described as passive control devices (passive flow restrictions). They influence the inflow from the reservoir into the well by the pressure drop caused by different permeability zones. [15]

Both AICV and ICD valves are placed in different permeability zones. The valve arrangements are described in Table 4-5.

[2] Inflow Control Device

[3] Autonomous Inflow Control Valve

Table 4-5 Case description

| Case | Description | Valves location description |
|---|---|---|
| 1. | B,D,F,H-ICD valves closed<br>Setpoint for Gas Liquid Ratio at Standard conditions (GLRST) is 200 | Closed valves alternatively located along the pipe with permeabilities at:<br>1000-2000-2000-2000-1000 mD |
| 2. | D,E,F,G-ICD valves closed<br>Setpoint for Gas Liquid Ratio at Standard conditions (GLRST) is 200 | Closed valves located just in the middle of the pipe(restriction of high permeability zones)with permeabilities at<br>2000,2000,2000,2000 mD |
| 3. | Open hole – all valves open<br>Setpoint for Gas Liquid Ratio at Standard conditions (GLRST) is 200 | All valves along the pipe are fully open along the pipe |
| 4. | A,B,C,D,E,F,G,H,I,J – AICV valves<br>Setpoint for Gas Liquid Ratio at Standard conditions (GLRST) is 200 | The valves are controlled by the PIDs with measured values readed by transmitters. AICV with relatively to 1% opening in closed position. |
| 5. | A,B,C,D,E,F,G,H,I,J – AICV valves<br>Setpoint for Gas Liquid Ratio at Standard conditions (GLRST) is 20 | The valves are controlled by the PIDs with measured values readed by transmitters. AICV with relatively to 1% opening in closed position. |

The completion of the pipe with valves, PID controllers, transmitters is shown in Figure 4-5 a) and b).

The packers, denoted as Valve-1 to Valve-9, close entyrely the annulus sectionwize in order to restrict inflow of fluid from a zone to another. The sources, denoted as NWSOUR-1 to NWSOUR-10 in each wellbore sectio, shows the fluid entrance in to the wellbore toward different each zone in the.

The leaks, denoted as Leak-1 to Leak-10, permit the fluid to enter the pipe from the wellbore through the ICD and AICV valves. Each leak is connected to the next neiboroughing section of the pipe annulus. However, in the pipeline fluid flows from one zone to another.

The details A and B shows a magnified picture of the end of the flowpath and the pipe. The transmitter and the PID controller placed on the flowpath controles the water and gas inflow into the ICD pipe arrangement due to the OLGA configuration of output values.

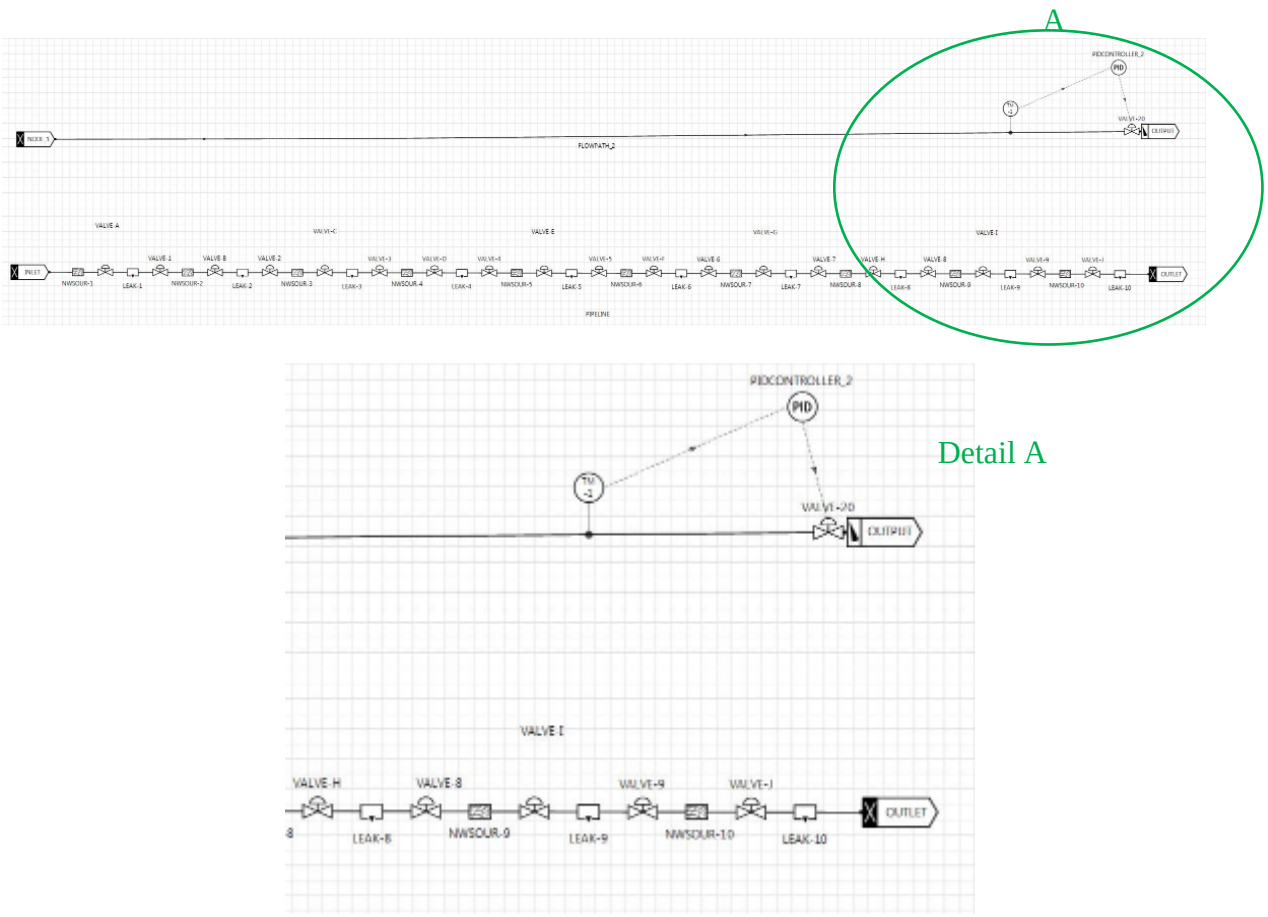


Figure 4-5 a) Model arrangement for ICD-valves arrangement

The AICV arrangement on the pipe controls the output using the transmitters placed in all sections of the wellbore.

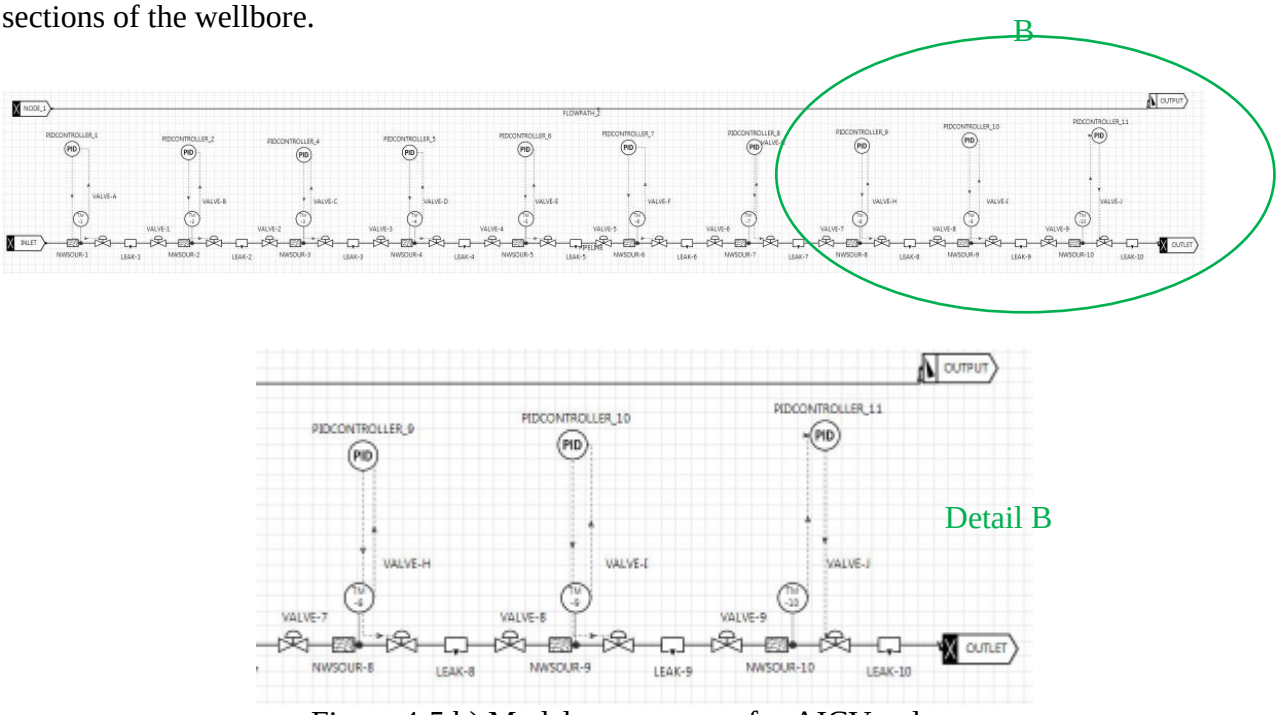


Figure 4-5 b) Model arrangement for AICV-valves

In order to evaluate the efficiency of water and gas extraction process over 300 simulation days, there was considerate following data:

- Total liquid volume flow, denoted as QLT ($m^3/d$)
- Gas volume, denoted as flow QG ($m^3/d$)
- Gas/Liquid ratio at standard conditions, denoted as GLRST (-)
- Accumulated water and gas volume before the gas breakthrough
- Total amount of water and gas accumulated after 300 days

Total liquid flow shows the production of water for each day and gives the base of calculation of total amount of extracted reservoir water after 300 days. Gas volume, considered at the reservoir conditions, is one of the most important criteria when the efficiency of the valve type is evaluated. The valves may assure great amount of extracted water but they can also permit a great amount of gas to flow into the pipe that ends up at the surface conditions in enormous amounts. The third criterion, gas/liquid ratio at standard conditions, shows clearly that this part of the process is very important to be considered from an economic point of view. Production of water and gas involves the ability of AICV and ICD valves to assure maximum amount of extracted water from the reservoir with as less as possible $CO_2$ extraction. The $CO_2$ storage in the aquifer depends on the effectivity of the valves.

## 4.3 Flow pressure as permeability dependent

The injected $CO_2$ is soluble in the formation water and the solubility is strongly dependent on temperature and pressure. In a water-wet reservoir, $CO_2$ will enter largest pores by replacing the formation water during the drainage. The $CO_2$ will rise upwards ($CO_2$ plume) and some of the gas will dissolve in the reservoir water.
The density of this solution is relatively higher than the original water. Higher density means a possible sinking of the $CO_2$-solution at the bottom of the reservoir.
The $CO_2$ in gas form will migrate up until it is stopped by the cap rock (seal). Because of this almost impermeable cap rock, assumed vertical permeability in the simulations is 200mD, the gas may migrate sideways along the wellbore and fill up the pipe through the valves.

An important factor is the pressure in the reservoir at the operating conditions. The injection of $CO_2$ simultaneously with water extraction must be controlled in order to assure that the pressure drop in the reservoir does not affect the sealing quality of the cap rock and the storage process has an optimal outcome.[7],[10],[20], [39]

Because of the pressure difference between the permeability zones, the water flow, in high quantities, will "push" even more toward the valves as shown in Figure 4-6.

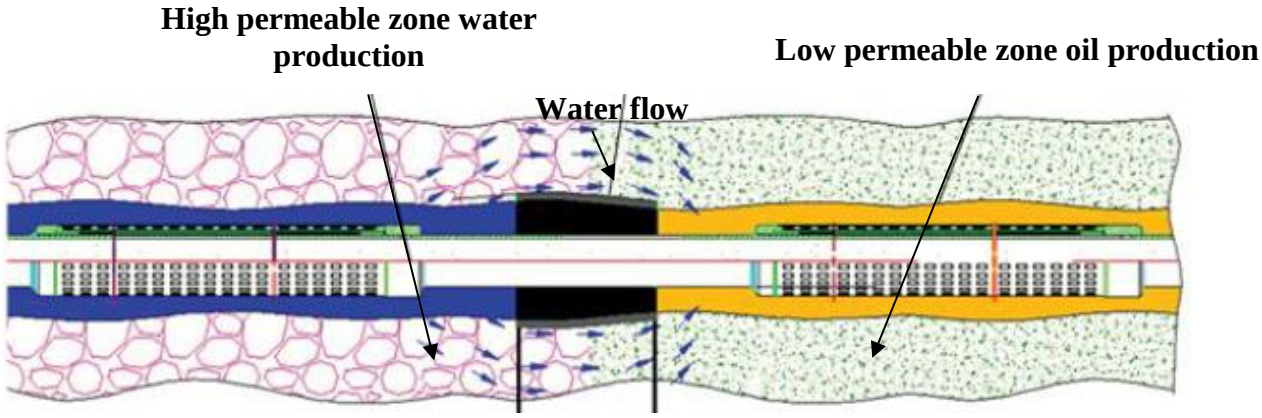


Figure 4-6 Water flow caused by permeability differences [40]

The gas breakthrough can indicate which valve arrangement is most efficient due to water extraction from the reservoir. This can help to track and stop the gas inflow as early as possible to avoid unnecessary water/gas separation costs at the surface.

# 5. Results and discussion

The conducted simulations indicate the importance of permeability distribution in the reservoir, the response of the valves during the water production and their capacity to assure an optimal extraction process when bi-production of $CO_2$ increases in time.

## 5.1 Gas distribution in modeled reservoir

Figure 5-1 - pictures plotted by using Techplot-software- show the gas saturation in the reservoir after the gas breakthrough and at the end of the simulation for each case as described in Table 4-5.

The high permeability zones in Case 2 are blocked by closed D, E, F, G- valves, see Figure 5-1a. The 2000 mD reservoir permeability here does not supply the flow into the pipe with either water or gas. Between these valves, along the pipe, the accumulated water and gas come from the precedent valves located in 1000 mD zones. The pressure exerted by water in the first three sections of the reservoir and the pressure drop varying between 8 and 10 bar between the flowpath and annulus result in a great inflow of reservoir water into the wellbore.

The gas concentration in this water flow increases slowly until the gas breakthrough appears after 42 days. The pale blue color indicates a low concentration of dissolved $CO_2$ in water.

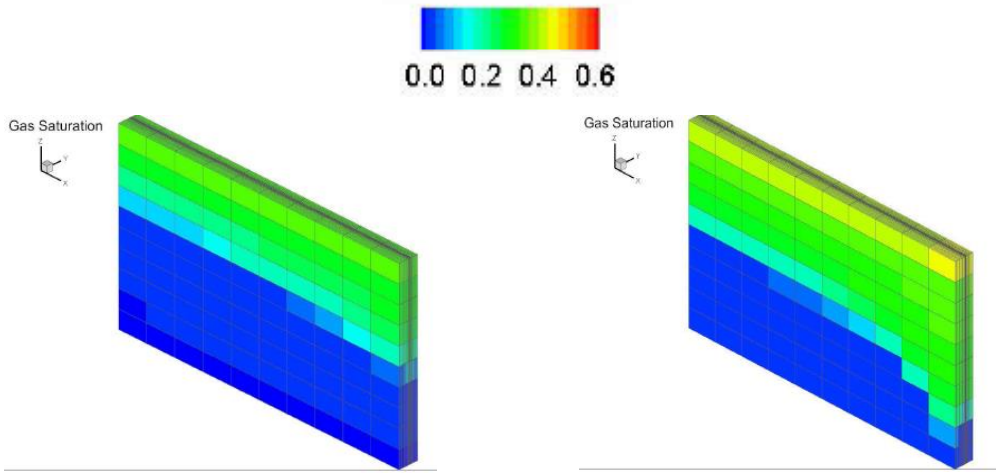


Gas distribution at breakthrough after 42 days  Gas distribution after 300 days

Figure 5-1 a) Gas distribution in the reservoir, Case 2

In Case 3, where all the valves are fully open, the gas breakthrough appears after 42 days too, but the gas concentration is much higher already from the gas breakthrough. The inflow of water and gas happens all the way through the wellbore. The density of water being higher than density of gas, the water comes earliest in the pipe. See Case 1 and Case 4 in Appendix B.
The higher concentrated gas occupies more and more space and migrates toward pipe. The gas saturation scale shows more accentuated colors on the top of the volume for this case.

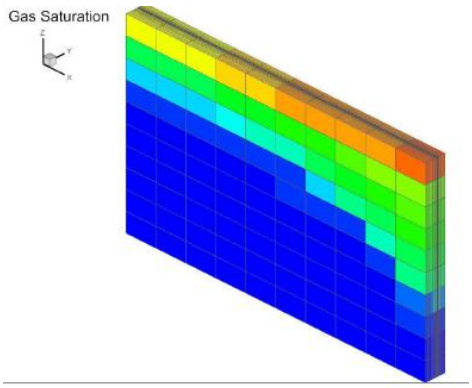


Gas distribution at breakthrough after 42 days

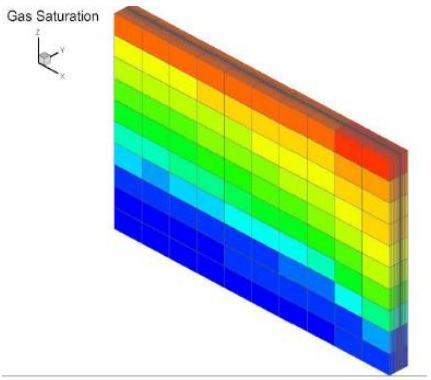


Gas distribution after 300 days

Figure 5-1 b) Gas distribution in the reservoir, Case 3

AICV valve in Case 5 permits the high viscous fluid (water with 0.287 cP viscosity at reservoir conditions) to go through while it chokes the low viscous flow ($CO_2$ with 0.02529 cP at reservoir conditions). This valve permits a much larger amount of water production before gas breakthrough. Then the valve starts to close for water after 42 days and gradually close down for water inflow. The water-$CO_2$ solution has higher density than the original formation water, which permits the enriched $CO_2$-solution to go through valve in greater amount than water. [16], [35]

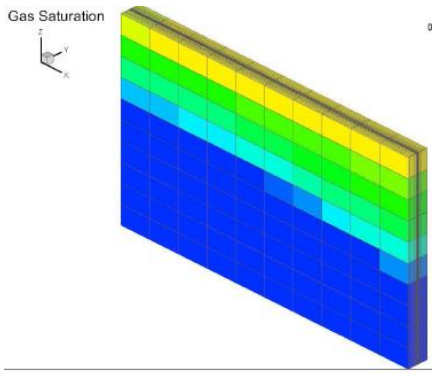


Gas distribution at breakthrough after 42 days

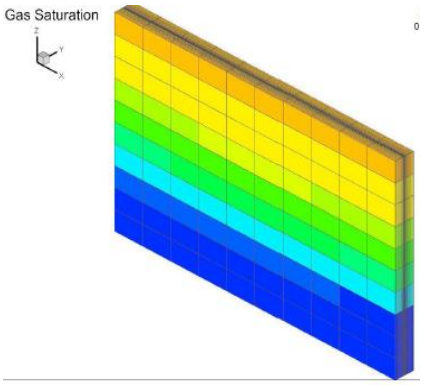


Gas distribution after 300 days

Figure 5-1 c) Gas distribution in the reservoir, case 5

The pressure difference may not vary too much between the sections before the gas breakthrough, see Figure 5-2.

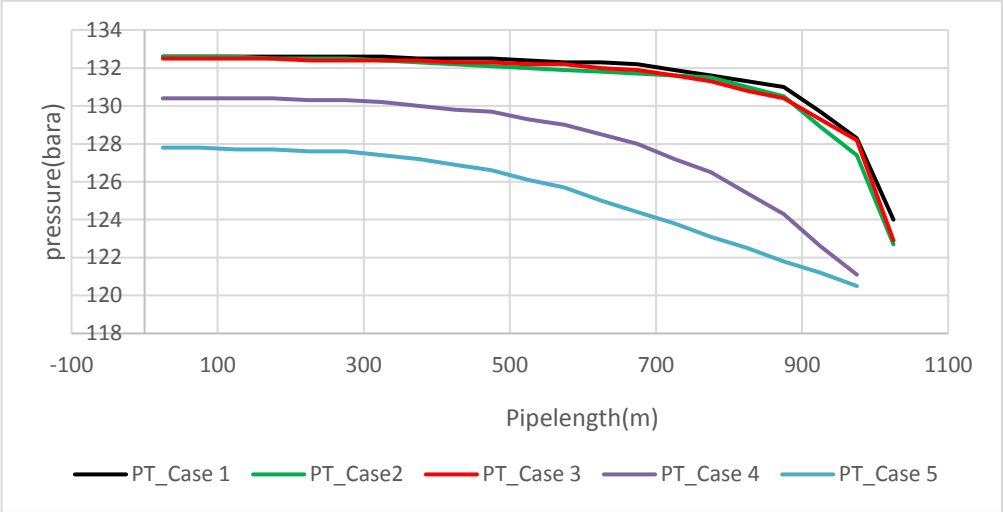


Figure 5-2 Pressure as a function of pipe length

## 5.2 Valve efficiency as a function of water and gas accumulation

An important idea in this work is to compare the valves competiveness to extract most reservoir water and less gas (assumed as $CO_2$) from the reservoir. The valve arrangements, as described in these five cases, may identify a god solution for the actual situation concerning water/gas production. This may be overviewed by using data described in Chapter 4.2.

These water accumulation patterns can be useful when considering the efficiency of the valves regarding water production over longer time than simulated, see Figure 5-3.

One of the most relevant aspect with respect to $CO_2$ storage capacity is the potential these five cases can show when production of water without gas is at the highest value. It is certainly worth the evaluation of the valve type when gas breakthrough in the wellbore may cause deficiencies in the process of water extraction and gas separation at the surface.

The gas breakthrough starts earliest in Case 3. A possible explanation may be that the all valves and packers in all permeability zones are fully open allowing both water and gas to flow into the pipe. The pressure difference that water flow creates from well bore towards pipe assure inlet of a quite large water production before the gas breakthrough.

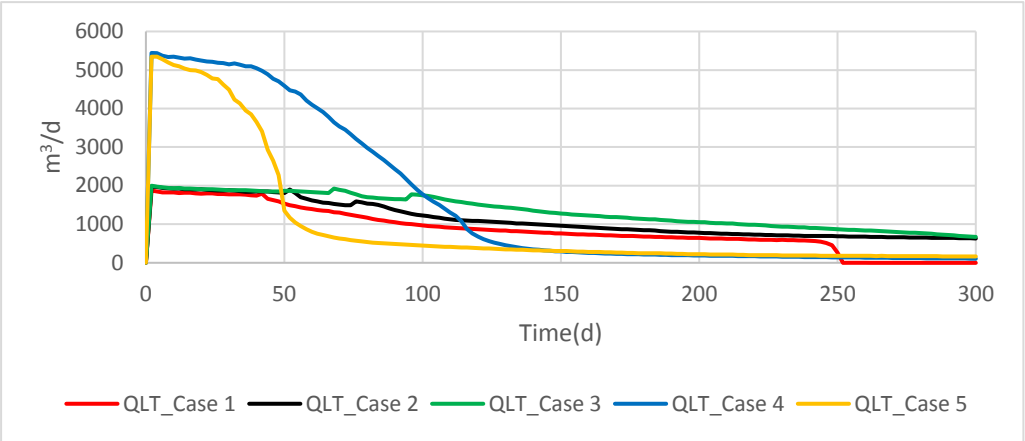


Figure 5-3 Total liquid volume flow as a function of time

The ICD valves allows water inflow and the total volume flow is controlled by a PID controller. This results in a much lower entrance of water right from the beginning of simulation. The differences between the valves capacities to permit water inflow can be explained by their positioning in variated permeability zones along the pipe.

These valves has low water extraction capacity compared with AICVs. The ICDs continue to produce lower amount of water even the gas inflow starts after 50 days.

The AICVs are fully open without restriction at the start until the setpoint is reached. The full opening and the viscosity difference between water-$CO_2$ solution and the gas makes these valves to allow a huge amount of water to flow into the pipe.

According to this figure, a maximum of total extracted liquid by using ICDs and AICVs is accumulated after 50 days by the AICV-valve, Case 4, when the gas reaches the pipe.

The ratio between the produced water amount before gas breakthrough and water amount after 300 days may indicate the efficiency of each case, as shown in Table 5-1.

Table 5-1 Water extraction efficiency as a function of accumulated water

| **Case** | **Accumulated water volume until the gas breakthrough ($m^3$)** | **Accumulated water volume after 300 days ($m^3$)** | **Case efficiency (%)** |
|---|---|---|---|
| Case 1 | 37 773 | 127 623 | 30% |
| Case 2 | 39 809 | 167 489 | 24% |
| Case 3 | 40 156 | 201 146 | 20% |
| Case 4 | 109 853 | 239 953 | 46% |
| Case 5 | 98 099 | 148 141 | 64% |

Figure 5-4 describes the performances and perhaps the challenges of using either ICD- or AICV-valves when gas amount coming into the pipe becomes too large. The cases can be evaluated as profitable or not over a longer period than simulated in this work. Furthermore, the gas/liquid ratio at standard conditions may exclude the cases, or valve-arrangements, where the ratio between water and gas when this ratio is not feasible as in Case 1, 4 and 5.

The AICV valves have the gas breakthrough at about same time but the gas amount collected over the same period, comparing with the ICD valves, is much larger. The AICV valve in Case 5 shows a better efficiency over a short time than all other valves. As shown in Figure 5-4, the gas inflow has a sudden rise over a very short period up to about 8-900 $m^3$/day after 60 days when the amount of gas increases very little and starts flattening out at the end of the simulation time

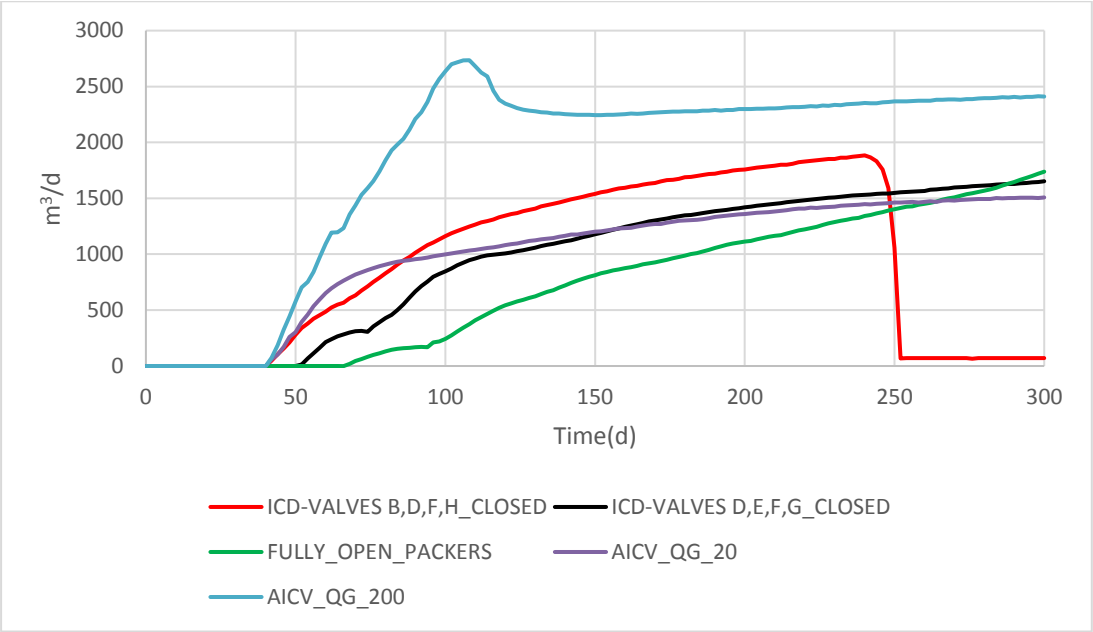


Figure 5-4 Total gas volume flow as a function of time

A reason for this may be the viscosity differences between the $CO_2$-brine solution and original formation water, as explained in Chapter 4.3.

Figure 5-5 shows that the produced gas at standard conditions is already in an overwhelming amount after 250 days for case 1, after100 days for Case 4, and after 200 days for Case 5, compared to Case 2 and Case 3.

In Case 3, the extracted gas amount exceeds the extracted water amount with 20% if the water production keeps going in 300 days. This is the smallest gas/fluid ratio of all cases.

A possible explanation can be that the all valves are open all the way permitting the water to flow into the pipe under the pressure difference between the wellbore and pipe.

The water accumulates under the reservoir pressure in the first two, three days when the pressure drop, in average of 8 bar, pushes the water flow from the wellbore into the pipe. The valve on the flowpath, controlled by the PID, minimize the inflow when gas accumulation increases.

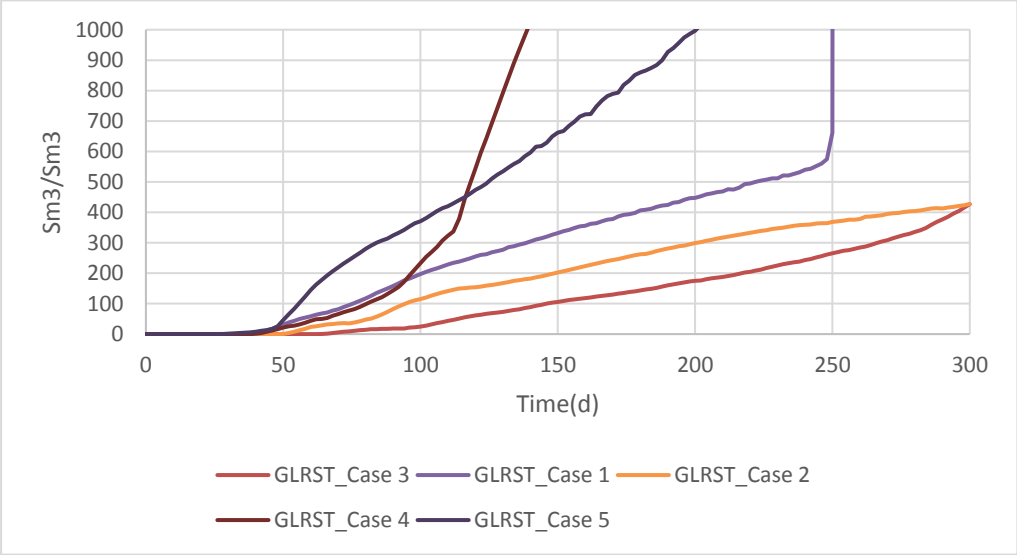


Figure 5-5 Gas/liquid ratio at standard conditions as a function of time

The other cases are controlled either by the valve arrangement in various permittivity zones, (where water pressure varies both from zone to zone and between the packer blockages) or by the settings of the autonomous valves.

Using the total amount of extracted water and gas during the simulation period, the efficiencies of the valve may not show remarcable benefits compared with each other when using either ICD or AICV valves. Case 4 produces largest volume of gas, 54 % of its production is $CO_2$ at the reservoir conditions, see Table 5-2.

Table 5-2 Extracted gas volume from total extracted fluid volume

| **Case** | **Total fluid volume after 300 days($m^3$)** | **Total gas volume after 300 days ($m^3$)** | **Gas volume percent of total extracted fluid after 300 days** |
|---|---|---|---|
| Case 1 | 269 790 | 142 175 | 53% |
| Case 2 | 314 418 | 146 930 | 47% |
| Case 3 | 312 511 | 111 364 | 20% |
| Case 4 | 518 040 | 278 086 | 54% |
| Case 5 | 301 857 | 153 716 | 51% |

## 5.3 Water and $CO_2$ extraction

The analyses of results for water extraction process, in order to insure increased storage capacity for $CO_2$, shows how the heterogeneity of the reservoir, the permeability dependency when closed/not closed ICD-valves and AICV-valves are functioning along the 1000 meters long pipe. The heterogeneity of the reservoir at the Utsira Sand formation is described as variating between sand and other layers of sediments that makes this reservoir very suitable to gas storage. The response of the valve models due to permeability characteristics of the reservoir and the assumed pressure and temperature conditions used in ROCX may contribute to an evaluation of the $CO_2$ storage potential in the aquifer.

**Case 1**- closed ICDs in different permeability zones- takes in a quite large amount of gas, about 142 176 $m^3$ over 250 days, while total amount of water is about 127 623 $m^3$. Gas/liquid ratio at standard conditions after 300 days ($Sm^3/Sm^3$), shows case 1 as not so efficient solution because of the $CO_2$ amount extracted up to the surface, see Table 5-3.

**Case 2**- closed ICDs just in the middle of highest permeability zone- takes in about 146 929 $m^3$ of gas over the same period as in case 1. Accumulated volume water in this case is about 167 489 $m^3$. Gas to liquid ratio at standard conditions after 300 days ($Sm^3/Sm^3$) is about 400 and the ratio may appear as constant with time (Table 5-3).

**Case 3** – fully open packers or "open hole" ICDs- along the pipe length shows an accumulated gas amount of 111 364 $m^3$ and water amount of approximately 201 146 $m^3$ over a 240 days period. Gas/liquid ratio is also about 400 as in Case 2 but it appears as rising further during 300 days.

**Case 4** – AICVs with setpoint of 200 for gas/liquid ratio at standard conditions - shows that the water amount is generally largest until the gas breakthrough, when this valve closes later compared with case 5, as shown in Figure 5-1. The total extracted amount of water is 239 953 $m^3$ and total accumulated gas is about 278 086 $m^3$. Gas to liquid ratio reaches enormous values quite early in the simulation. If the water production in shortest time is the main issue, this case may be a good solution.

**Case 5** - AICVs with setpoint of 20 for gas/liquid ratio at standard conditions – is shown as fairly god regarding the totally amount of extracted gas and water even if the advantages of using this valve may be evaluated for a short period of time. This valve can assure a total amount of water for about 148 141 $m^3$ and 153 716 $m^3$ of $CO_2$. This valve starts closing for gas and water earliest of all other cases but still "recovering" from about 5000 $m^3$/day to 2000 $m^3$/day water in a shortest time.

Accumulation of water and gas is shown in Table 5-3.

Table 5-3 Comparation of accumulated water volume until the gas breakthrough and accumulated water volume in total after 300 days

| **Case** | **Accumulated water volume until the gas breakthrough ($m^3$)** | **Accumulated water volume after 300 days ($m^3$)** | **Accumulated gas volume after 300 days($m^3$)** | **Gas to liquid ratio at standard conditions after 300 days($Sm^3/Sm^3$)** |
|---|---|---|---|---|
| Case 1 | 37 773 | 127 623 | 142 175 | Only gas |
| Case 2 | 39 809 | 167 489 | 146 930 | At least 400 times more gas than water |
| Case 3 | 40 156 | 201 146 | 111 364 | About 400 times more gas than water |
| Case 4 | 109 852 | 239 953 | 278 086 | Only gas |
| Case 5 | 98 099 | 148 141 | 153 716 | Only gas |

Calculated total $CO_2$ storage capacity of the reservoir, with dimensions as described in Chapter 4.1, is about 0.223 Mt for $CO_2$ at reservoir conditions, see equation [3-3]. To assure a concrete storage capacity, the geological data should be able to map the reservoir more accurately. Assuming a total replacement of the produced water with $CO_2$, the efficiency of each case can be calculated by using the total amount of gas that can replace produced water, total amount of gas that can replace the produced water until the gas breakthrough and the total amount of gas extracted in each case.

The large amount variation in produced water and gas from Case 1 to Case 5 does not insure a particular case with large distinguished profit.

The maximum water production before gas breakthrough, the efficiency related to total accumulated water and the gas/liquid ratio at standard conditions over the whole simulation period can be a criteria that can give a better approach to a practical solution, see Figure 5-6.

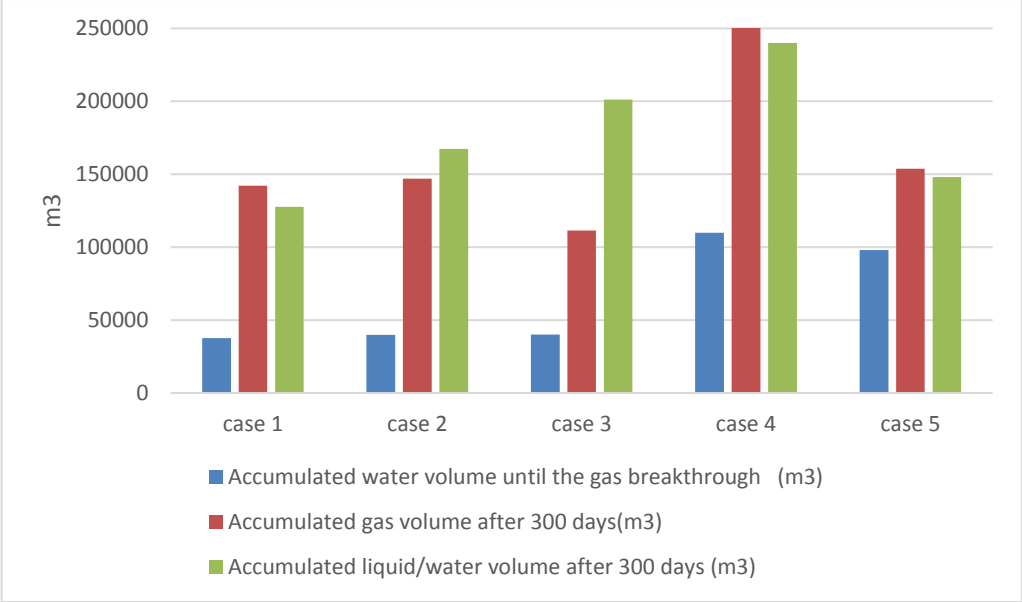


Figure 5-6 Water and gas production for all cases

Accumulated water and gas appears to follow each other's values fairly close in almost all cases as Figure 5-7 shows but the main criteria such as major water production and minor gas production separates clearly Case 2, 3  Case 5 from the other cases.

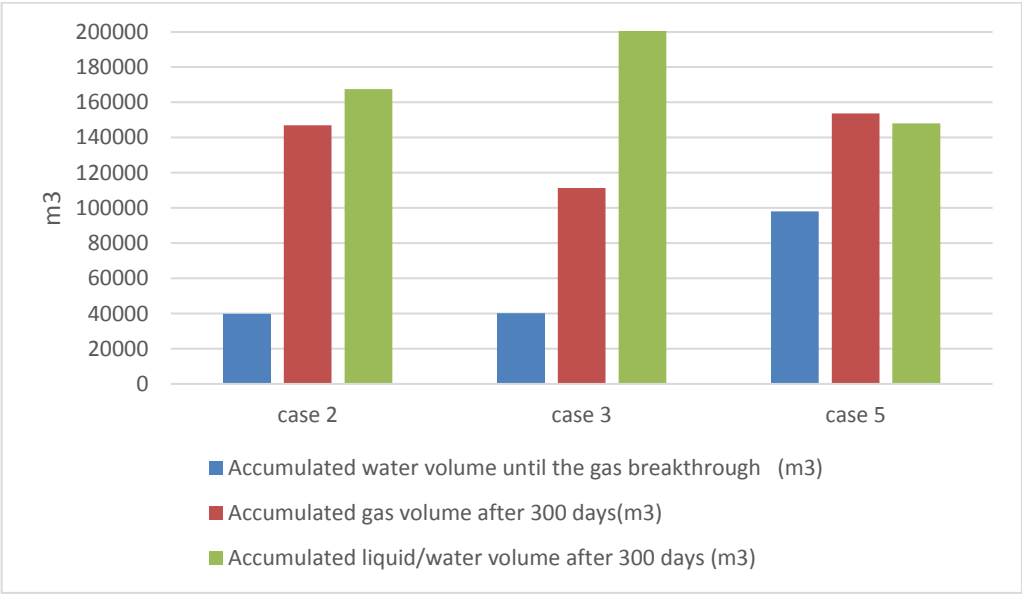


Figure 5-7 Water and gas production for Case 2, 3 and 5

## 5.4 Gas breakthrough

The gas breakthrough in Case 2 appears about eight days later along with 40% less amount of water than in Case 5 before the gas breakthrough, see Figure 5-8.

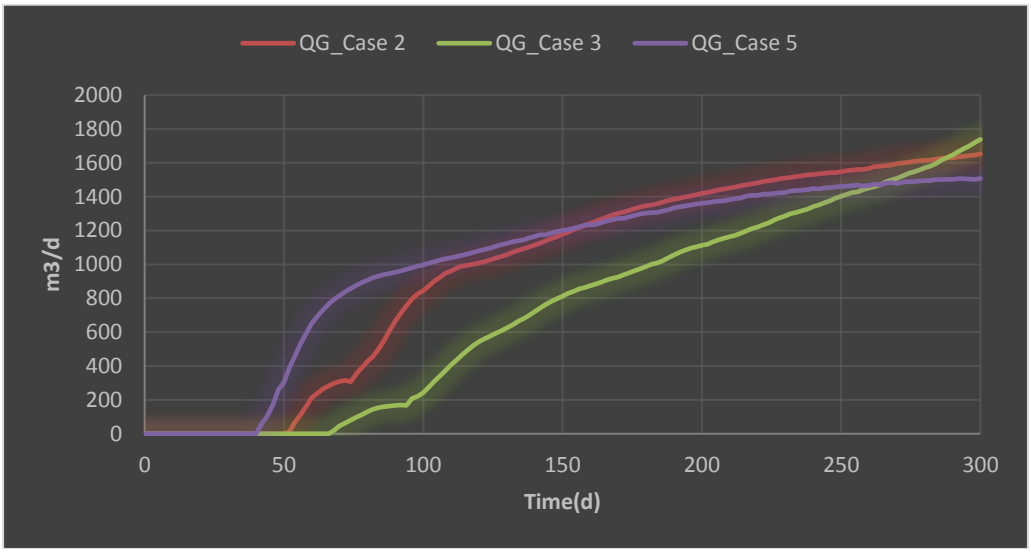


Figure 5-8 Gas breakthrough Case 2, 3 and 5

The valves in Case 2 permits the water inflow only from lower permeability zones but under the restrictions from the valve on the flowpath while the valves in Case 5 are fully open to high density fluid on whole pipelentgh. Case 3 has all ICDs operating along with open packers, which allows the water from high permeability zones to enter the pipe (pressure) and increase the pressure over the neighboring low permeable zone. Once the water has "released" more space from the reservoir pores, the $CO_2$ with much lower density becomes more mobile and pushes a front of brine mixed with $CO_2$ into the wellbore. The gas flows, now in larger amount, builds up both pressure and inflow near the valve on the flowpath (between 850 and 1000 meters), as shown in Figure 5-9.

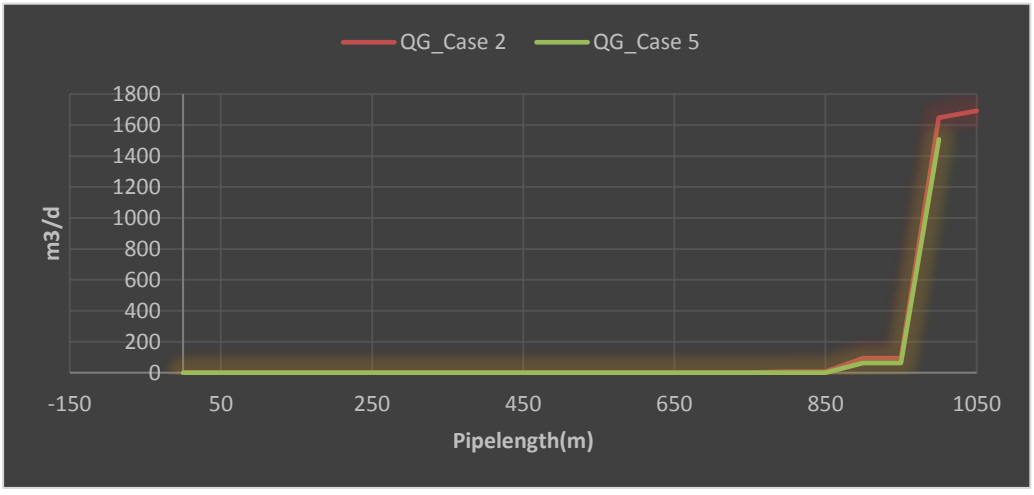


Figure 5-9 Schematic of gas breakthrough Case 2 and Case 5 as function of pipelentgh

## 5.5 Storage potential

The volume of extracted water may be replaced with carbon dioxide considering density difference at the reservoir conditions and the theoretical storage capacity of a reservoir volume calculated with equation [3-4] in Chapter 3.2, see Appendix C.
Taking in account the assumed porosity for Utsira and the density values for water and $CO_2$ at 100 °C and 130 bar, the total amount of $CO_2$ possible to store for all cases is shown in Table 5-4.
A clear advantageous solution it may not be possible to apply when long-term production is a parameter. All cases have almost similar high extracted gas rates in this matter.

Table 5-4 $CO_2$ storage capacities in the reservoir

| **Case** | **Total amount of extracted $CO_2$ during water production(Mt)** | **Total possible $CO_2$ amount to store at reservoir conditions after 300 days(Mt)** | **Possible $CO_2$ amount to store until gas breakthrough at the reservoir conditions(Mt)** | **Percentage of more extracted $CO_2$ than produced water (due to total amount of extracted fluid) ( %)** |
|---|---|---|---|---|
| Case 1 | 0.039 | 0.035 | 0.010 | 53 |
| Case 2 | 0.040 | 0.046 | 0.011 | 47 |
| Case 3 | 0.030 | 0.055 | 0.011 | 56 |
| Case 4 | 0.077 | 0.066 | 0.030 | 54 |
| Case 5 | 0.042 | 0.041 | 0.027 | 51 |

The advantage of using Case 4 or Case 5 is may be even clearer now because of the possibility to minimize or shut down the water production when gas flows in. In the same time the AICV valve arrangement in Case 5 insure almost the largest amount of $CO_2$ of 0.027 Mt $CO_2$ until gas breakthrough comparing with the other cases.
The theoretical storage capacity calculated with equation [3-3] shows that Case 4 and Case 5 covers 13.5% respectively 12% of this potential storage (before the gas breakthrough) and 30% respectively 19% of the modeled volume after 300 days production, see expression *[C-8]* in Appendix C for the other cases.

# 6. Cost estimation

Carbon capture and sequestration involves separation, transport and storage processes with available technologies that influence the economical aspect when storage of $CO_2$ is cost evaluated.

The storage of $CO_2$ in saline aquifers includes the compression and injection due to assure as large as possible amount of gas offshore. The $CO_2$-EOR technologies has a huge economical gain unlike injecting of $CO_2$ only for storage in depleted oil reservoir and saline aquifers. The $CO_2$ revenues represents the economic benefit from the emission taxes, see Table 6-1. They were assumed as 55 USD/t $CO_2$. Considering reusing of already existing infrastructure in depleted oil fields or pilot project costs, such as Sleipner storage project at the Utsira Formation with included monitoring, the current estimates lie in the range of 50 to 100 USD /t $CO_2$ of stored $CO_2$. The costs in Table 6-1 are set to an average of 80 USD/t $CO_2$. These costs are mainly based on reusing the $CO_2$ at the same facilities and location (Sleipner project) where compression to 200-300 bar and gas reinjection rise the operational costs. [41], [42], [43]

As the economic review on Table 6-1 shows, all five simulated cases have large expenditures due to the bi-production of $CO_2$. In the same time, it is worthwhile to evaluate storage capacity before gas breakthrough. Large water amounts produced by using Case 4 and 5 before gas breakthrough may assure a storage capacity up to 0.030 Mt $CO_2$ within about 50 days. It means that in these cases, the reservoir may store about 14% of its capacity. This gives a $CO_2$ income of about 1.5-1.6 million USD for only 50 days of water extraction.

Table 6-1 Total costs $CO_2$ extracted from the reservoir

| **Case** | **Total amount of extracted $CO_2$ during water production (Mt)** | **Total cost of $CO_2$ compression and reinjection of total amount extracted gas (80 USD/tonne) assumed as CCS costs, USD** | **Revenues $CO_2$ for storage capacity in aquifer after 300 days water extraction ($55USD/t CO_2$), USD** | **Revenues $CO_2$ for storage capacity in aquifer until gas breakthrough ($55USD/ t CO_2$), USD** |
|---|---|---|---|---|
| Case 1 | 0.039 | -2,112 mill | +1.925 mill | 0.55 mill |
| Case 2 | 0.040 | -2,180 mill | +2.530 mill | 0.605 mill |
| Case 3 | 0.030 | -1,656 mill | +3.025 mill | 0.605 mill |
| Case 4 | 0.077 | -4,128 mill | +3.630 mill | 1.650 mill |
| Case 5 | 0.042 | -2,292 mill | +2.255 mill | 1.5 mill |

Other OPEX[4] costs such as maintenance, electricity, monitoring etc., are not detailed here. A basic calculation of benefits based only on gas processing costs shows that Case 4 costs twice as much as the other cases only on compression and injection costs. On the other hand, if the costs are analyzed only from the storage capacity of the reservoir before gas breakthrough, Case 4 it seems most beneficiary. Case 4 comes quite close to Case 5 in the matter of storage capacity but is about double as much expensive as Case 5, see Table 6-1.

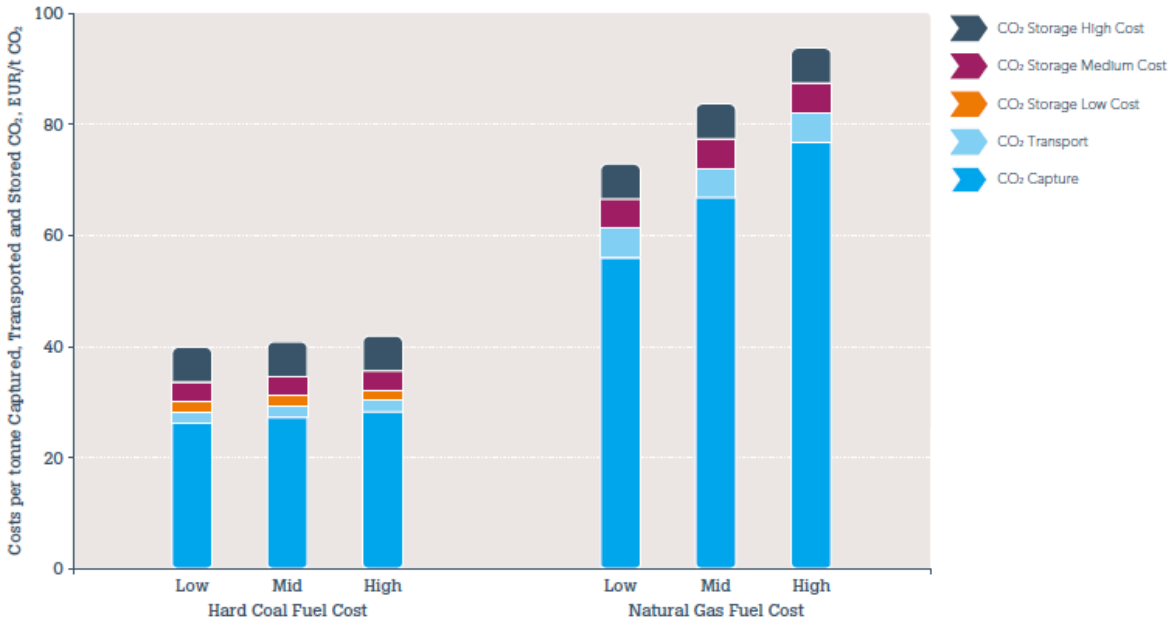


Figure 6-1 €/tCO2 captured for integrated CCS projects with Low, Middle and High Fuel costs [43]

Figure 6-1 concludes that $CO_2$ capture, transport and storage costs calculated per tonne basis are more expensive for natural gas than for coal. The reinjection of produced $CO_2$ is then an important issue. These basic costs from Figure 6-1 may give an overview of expenses when the gas already produced has to be restored in the reservoir, see Appendix D.

[4] OPEX – Operating expenditure (The ongoing costs accompany pays to run its basic business)

# 7. Conclusion and suggestion to further work

In order to find a possible beneficent solution, the near-well simulation software ROCX and OLGA war used. The reservoir conditions were assumed close to Utsira Sand's aquifer reservoir with high permeability, uniformly variated heterogeneity in the horizontal direction and low permeability in the vertical direction.

Simulated water extraction from the reservoir was conducted using five different arrangements of valves and two valve types.

Calculation of $CO_2$ storage potential was based on the idea of removal of the reservoir water in order to replace it with $CO_2$ using ICD- and AICV valves along the pipe.

The comparison between ICD and AICV valves functions in different permeability zones shows that the reservoir characteristics have a great impact due to both produced water amount and gas breakthrough.

In the same time, the capability of the valves to respond to the water inflow, as an advantage, and gas inflow as a disadvantage, concludes that the choice of a particular solution is a matter of both valve type and the economical aspect related to water treatment costs at the surface.

ICD valves have quite good performance in water production. This valve type delivers an accumulated water volume up to 201 146 $m^3$ but with a highest gas production of 53% of total accumulated fluid volume.

Connecting ICD valves as case 1, 2 and 3 describe, controlled by a PID on the wellbore, the accumulated water volumes shows quite large differences. The gas breakthrough appears later than in AICV connection but the water production is much less right from the start.

Water extraction efficiencies have quite close values to each other, between 20% and 30% while the gas production varies from 20% to 53% of total extracted fluid.

Production time should be a very important evaluation factor in order to increase $CO_2$ storage capacity in the aquifer. Produced water before the gas breakthrough (before 42 and 60 days for each case), may release as much as 37 773 $m^3$ and up to 109 852 $m^3$ volume which means a $CO_2$ storage capacity from 0.010 Mt up to 0.011 Mt.

AICV valves can gather about 148 141$m^3$ water and mostly 239 953$m^3$. This is about 54% of all extracted fluid from the modeled reservoir volume. These valves delivers the greatest volume of reservoir water in shortest period of time, before the gas breakthrough. If long-term production is an issue, AICV valves may not be as profitable as ICDs in case 3 because of the huge accumulated volume of gas of about 278 086 $m^3$.

The effectivity of each case relies on the capacity to accomplish the largest storage capacity of $CO_2$ in the reservoir without adding significant costs. Extraction of gas during the water production as a bi-process cause large economic consequences. The choice of the optimal solution among these five cases depends on the long term financial issues such as lower storage costs, new development projects, oil and energy price, maintenance and transport

The investment costs regarding the gas injection technology varies from reservoir to reservoir. $CO_2$ injection for EOR combined with storage is calculated assuming that the equipment is already in place and reused.

This study focuses on relationship between valves configuration and the reservoir properties but this can be extended in order to see how the location of the valves, their open/closed configurations may assure a better water production with less gas extraction.

A comparative study of the ability to close the valves at an optimal time before gas breakthrough may give even better benefits when greater reservoir water production assure larger $CO_2$ storage capacity.

# References


1. R.J. KLAPPERICH, R.M. COWAN, C.D. GORECKI, G. LIU, J.M. BREMER, Y.I. HOLUBNYAK, J.L. LABONTE, N.S. KALENZE, D.J. STEPAN, D.J. KNUDSEN, E.N. STEADMAN, D. SAINI, J.A. HARJU, L.S. BOTNEN, L. BASAVA-REDDI and A.McNEMAR, **IEAGHG Investigation of Extraction of Formation Water from CO2 Storage**, *Energy & Environmental Research Center, University of North Dakota IEAGHG, The Orchard Business Centre, U.S. Department of Energy, National Energy Technology Laboratory*

2. E. GHOODJANI, S.H. BOLOURI, **Experimental study and calculation of CO2-oil relative permeability**, *Sharif University of Technology, Tehran, Shahid Bahonar University, Kerman, Iran, Received November 23, 2010, Accepted May 15, 2011*

3. R.A. CHADWICK1, S. HOLLOWAY1 , G.A. KIRBY1 , U. GREGERSEN2 , P.N. JOHANNESSEN, **The Utsira Sand, Central North Sea – An assessment of its potential for regional $CO_2$ disposal**, *British Geological Survey (BGS), Geological Survey of Denmark and Greenland (GEUS),* https://www.sintef.no/globalassets/project/ik23430000-sacs/publications/chadwick_et_al_ghgt5.pdf

4. SAIF S. AL SAYARI **The Influence of Wettability and Carbon Dioxide Injection on Hydrocarbon Recovery**, *Department of Earth Science and Engineering Imperial College London, September 2009*

5. PER E. S. BERGMOA, ALV-ARNE GRIMSTAD, ERIK LINDBERG, FRIDTJOF RIIS, WENCHE T. JOHANSEN, **Exploring geological storage sites for $CO_2$ from Norwegian gas power plants: Utsira South**, *SINTEF Petroleum Research, Norwegian Petroleum Directorate*

6. **Calculation of CO2-density for different temperature and pressure** http://www.peacesoftware.de/einigewerte/co2_e.html

7. STEFAN IGLAUER, **Dissolution Trapping of Carbon Dioxide in Reservoir Formation Brine – A Carbon Storage Mechanism**, *Curtin University, Department of Petroleum Engineering, ARRC Building, Australia*

8. LUDMILA VESJOLAJA, AMBROSE UGWU, ARASH ABBASI, EMMANUEL OKOYE, BRITT M.E. MOLDESTAD, **Simulation of CO2 for Enhanced Oil Recovery**, *Department of Process, Energy and Environmental Technology, University College of Southeast Norway, Porsgrunn, Norway*

9. FRIDTJOF RIIS AND COWORKERS, **Attributes of a CO2 storage complex. CO2 in the subsurface, injectivity, capacity, trapping mechanisms and types of traps**, *Presentation at CCOP training course, August 20-22, 2013*

10. ERIK LINDENBERG, JEAN-FRANCOIS VUILLAUME, AMIR GHADERI, **Determination of the CO2 storage capacity of the Utsira formation**, *SINTEF Petroleum Research, Trondheim, Norway*

11. ANGELA GOODMAN, ALEXANDRA HAKALAA, GRANT BROMHAL, DAWN DEEL, TRACI RODOSTA, SCOTT FRAILEYC, MITCHELL SMALL, DOUG ALLENE, VYACHESLAV ROMANOVA, JIM FAZIOA, NICOLAS HUERTAA, DUSTIN McINTYRE, BARBARA KUTCHKOA, GEORGE GUTHRIEA, **International Journal of Greenhouse Gas Control, U.S. DOE methodology for the development of geologic storage potential for carbon dioxide at the national and regional scale**

12. KEWEN LI AND ROLAND N. HORNE, **Comparison of methods to calculate relative permeability from capillary pressure in consolidated water-wet porous media**, 4 June 2006.

13. BRITISH GEOLOGICAL SURVEY, **The underground disposal of carbon dioxide**, *Edited by S Holloway Contract No JOU2 CT92-003 1 FINAL REPORT, http://nora.nerc.ac.uk/502763/1/Joule%20II%20final%20report.pdf*

14. TECHNICAL STUDY, **Development of storage coefficients for carbon dioxide storage in deep saline formations,** *Report No. 2009/ 13*

15. JEANETTE GIMRE, MASTER'S THESIS, **Efficiency of ICV/ICD systems**, *University of Stavanger, 2012*

16. MARK McBRIDE-WRIGHT, GEOFREY C. MAITLAND AND J. P. MARTIN TRUSLER, **Viscosity and Density of Aqueous Solutions of Carbon Dioxide at Temperatures From (274 to 449) K and at Pressures up to 100 MPa,** *Qatar Carbonates and Carbon Storage Research Centre (QCCSRC), Department of Chemical Engineering, Imperial College London, United Kingdom.*

17. **Relative Permeability Correlations,**
http://www.fekete.com/SAN/WebHelp/FeketeHarmony/Harmony_WebHelp/Content/HTML_Files/Reference_Material/Calculations_and_Correlations/Relative_Permeability_Correlations.htm

18. Y. WANG Z. CHEN, V. MORAH, R. J. KNABE and M. APPEL, **Gas phase relative permeability characterization on tight gas samples**, *Shell International E & P, Inc., Houston, USA*

19. **Relative permeability**,
https://infohost.nmt.edu/~petro/faculty/Engler524/PET524-RelativePermeability-ppt.pdf

20. M. BENTHAM and G. KIRBY, **$CO_2$ Storage in Saline Aquifers**, *BGS, Kingsley Dunham Centre, Keywork, Nottingham, United Kingdom*

21. STEFAN BACHU, **Drainage and imbibition CO2/brine relative permeability curves at in situ conditions for sandstone formations in western Canada**, *Innovates Technology Futures*

22. N.M. BURNSIDE, M. NAYLOR, **Review and implications of relative permeability of CO2/brine systems and residual trapping of $CO_2$**, *Scottish Carbon Capture and Storage, School of Geosciences, University of Edinburgh, United Kingdom*

23. **Wettability in Oil and Gas Reservoirs,**

http://www.epgeology.com/reservoir-engineering-f10/wettability-oil-and-gas-reservoirs-t5978.html

24. MAHESH PRIVANKARA EDIRIWEERA, **Near well simulations of heavy oil reservoir with water drive**, *Master's Thesis 2014, Telemark University College, Faculty of Ttechnology*

25. V.T.H. PHAM, F. RIIS, I.T. GJELDVIK, E.K. HALLAND, I.M. TAPPEL, P. AAGAARD, **Assessment of CO2 injection into the south Utsira-Skade aquifer, the North Sea, Norway**, *Norwegian Petroleum Directorate, Department of Geosciences, University of Oslo, Norway*

26. ROSALIND WADDAMS, **Calculation of storage capacity for $CO_2$ in North Sea saline reservoirs**, 2008, på oppdrag fra Statens forurensningstilsyn

27. TOR ELLIS AND COWORKERS, *Stavanger-Norway,* ALPAY ERKDAL, *Texas-USA,* GORDON GOH, *Kuala Lumpur-Malaysia,* ANNE GERD RAFFN, *England,* **Inflow Control Devices – Raising profiles**

28. SAMUEL HÖLLER, PETER VIEBAHN, **Assessment of CO2 Storage Capacity in Geological Formations of Germany and Northern Europe**, *Wuppertal Institute for Climate, Environment and Energy, Germany*

29. WAEL ABDALLAH, *Alberta, Canada*, JILL BUCKLEY, *New Mexico, USA,* ANDREW CARNEGIEK, *Kuala Lumpur, Malaysia,* JOHN EDWARDS, BERND HEROLD, *Muscat, Oman,* EDMUND FORDHAM, *Cambridge, England,* ARNE GRAUE, *University of Bergen, Norway,* TAREK HABASHY, NIKITA SELEZNEV, CLAUDE SIGNER, *Boston, Massachusetts, USA,* HASAN HUSSAIN, *Petroleum Development Oman,* BERNARD MONTARON, *Dubai, UAE,* MURTAZA ZIAUDDIN, *Abu Dhabi, UAE,* **Fundamentals of Wettability**

30. **Wettability in Oil and Gas reservoirs**

http://www.epgeology.com/reservoir-engineering-f10/wettability-oil-and-gas-reservoirs-t5978.html

31. BERT METZ, OGUNLADE DAVIDSON, HELEEN DE CONINCK, MANUELA LOOS, LEO MEYER, **IPCC Special Report on Carbon Dioxide Capture and Storage**,

*Prepared by Working Group III of the Intergovernmental Panel on Climate Change, Cambridge University Press, Cambridge, United Kingdom and New York, NY, USA*

32. GLENN-ANDRÉ DÅTLAND KVINGE, En eksperimentell studie av $CO_2$ lagring i sandstein og kalkstein med bruk av ulike avbildningsteknikker, **Masteroppgave i reservoarfysikk**, *Institutt for fysikk og teknologi, Universitetet i Bergen, November 2012*

33. ODD MAGNE MATHIASSEN, **$CO_2$ as Injection Gas for Enhanced Oil Recovery and Estimation of the Potential on the Norwegian Continental Shelf**, *NTNU – Norwegian University of Science and Technology*, *Department of Petroleum Engineering and Applied Geophysics*

34. NORWEGIAN PETROLEUM DIRECTORATE**, Compiled CO2 atlas for the Norwegian Continental Shelf,** http://www.npd.no/en/Publications/Reports/Compiled-CO2-atlas/

35**. Calculation of water and CO2-density for different temperature and pressure,** http://www.peacesoftware.de/einigewerte/co2_e.html

36. NORA CECILIE IVARSDATTER FURUVIK**, Simulation of oil production and CO2-distribution in carbonate**, *Telemark University College 2106*

37. FRANK JAHN, MARK COOK AND MARK GRAHAM, **Hydrocarbon Exploration and Production,** p.159-160, *Tracs International Consultancy Ltd, Aberdeen, UK*

38. HANS-EMIL BENSNES TORBERGSEN, **Application and Design of Passive Inflow Control Devices on the Eni Goliat Oil Producer Wells**, *Master's Thesis, University of Stavanger, 2010*

39. ALIF BE, **Multiphase Flow in Porous Media with Emphasis on CO2 Sequestration,** *Dissertation for the degree philosophiae doctor (PhD) at the University of Bergen, 2011*

40. BEILING PEI, *China University of Petroleum Beijing,* WU LONG BO CHEN, *Northwest Bureau of Sinopec Urumqi, China,* SONGMEI ZHANG JIANWEI DI, *Anton Bailin Oilfield Technology Co. Ltd.Beijing,* **ICD-packer completion reduces water in China's Jidong oil field,** *2016*

41. INTERNATIONAL ENERGY AGENCY, **CO2 CAPTURE AND STORAGE A key carbon abatement option (pp 16, 88-107)**, *2008*

42. HAVVA BALAT, CAHIDE OZ, **Technical and Economic Aspects of Carbon capture and Storage - A Review, ENERGY EXPLORATION & EXPLOITATION,** *Volume 25, Number 5, 2007, pp.357-392*

43. **The Costs of CO2 Capture, Transport and Storage,** *Post-demonstration CCS in the EU of $CO_2$ Capture, European Technology Platform for Zero Emission Fossil Fuel Power Plants, July 2011*

# Appendices

Appendix A: Task description

Appendix B: Simulation of water and gas extraction in Utsira-conditioned reservoir

Appendix C: Calculations of $CO_2$ storage potential

Appendix D: Cost calculations

# Appendix A

University College of Southeast Norway

Faculty of Technology, Natural Sciences and Maritime Sciences, Campus Porsgrunn

## FMH606 Master's Thesis

**Title**: Study of $CO_2$ storage in oil reservoirs and aquifers

**HSN supervisor**: Britt M. E. Moldestad, Nora C. I. Furuvik

**External partner**: InflowControl AS, Haavard Aakre

**Task background**:

$CO_2$ is used for Enhanced Oil Recovery (EOR) in fields with high amount of residual oil. In addition to using $CO_2$ for EOR, it is crucial to store $CO_2$ to avoid the large contribution to global warming due to $CO_2$ emission. Norway has used the Utsira formation for storage of $CO_2$ from the Sleipner reservoir since 1996. The Utsira formation is a 300 km long field consisting of porous sand stone and estimates show that the formation has the capacity to store 40 billion ton $CO_2$ over a period of 300 years. Mature oil and gas reservoirs and underlying aquifers are considered as the future solution for $CO_2$ storage. It is predicted that the North Sea has the capacity to store $CO_2$ from all the coal power plants and other large $CO_2$ sources in Europe. A better understanding of the storage capacity and suitability for $CO_2$ storage in reservoirs and aquifers are needed.

**Task description**:

The project will focus on:

1. Study related to $CO_2$ storage capacity on the Norwegian shelf.
2. Calculations related to $CO_2$ storage.
3. Simulation of $CO_2$ injection and storage. Different simulation tools are available.
4. Cost estimation.

**Practical arrangements**:

Necessary software will be provided by TUC.

**Student category**: PT. It is beneficial to have some knowledge about reservoir and near well simulation.

**Signatures**:

Student (date and signature): Loreana Gjeden

Supervisor (date and signature): Britt Moldestad

Nora Furuvik

Address: Kjølnes ring 56, NO-3918 Porsgrunn, Norway. Phone: 35 57 50 00. Fax: 35 55 75 41.

# Appendix B

Simulation of water and gas extraction in Utsira-conditions reservoir

a. Gas breakthrough in time for Case1, Case 3, Case 4 and Case 5:

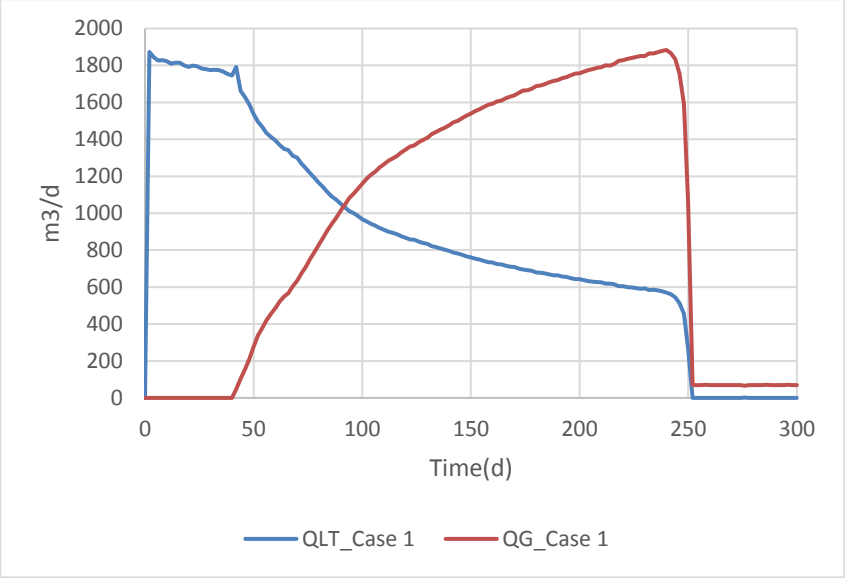


Figure B-1: Gas breakthrough for Case 1

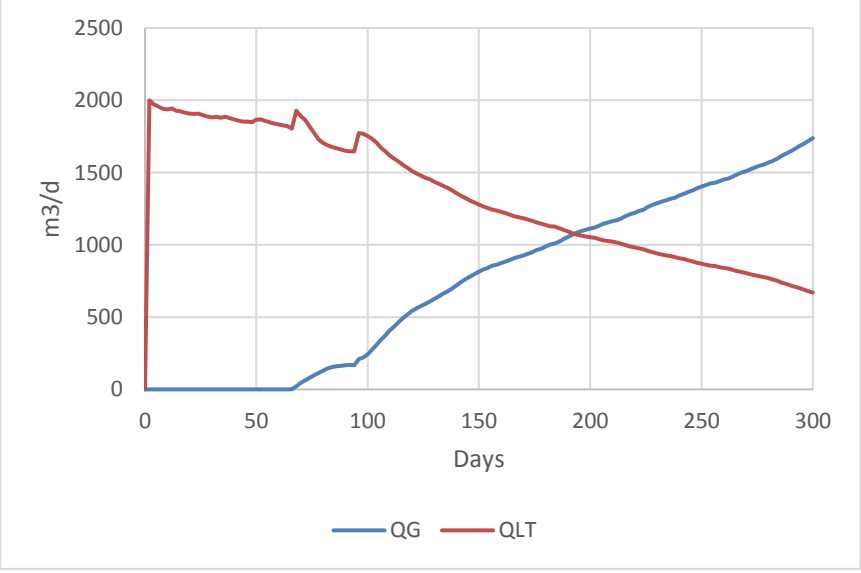


Figure B-2: Gas breakthrough for Case 3

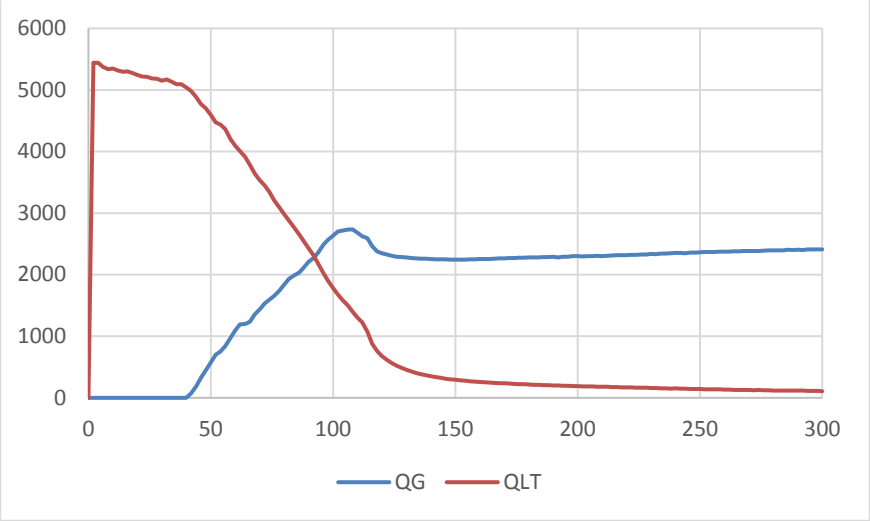


Figure B-3: Gas breakthrough for Case 4

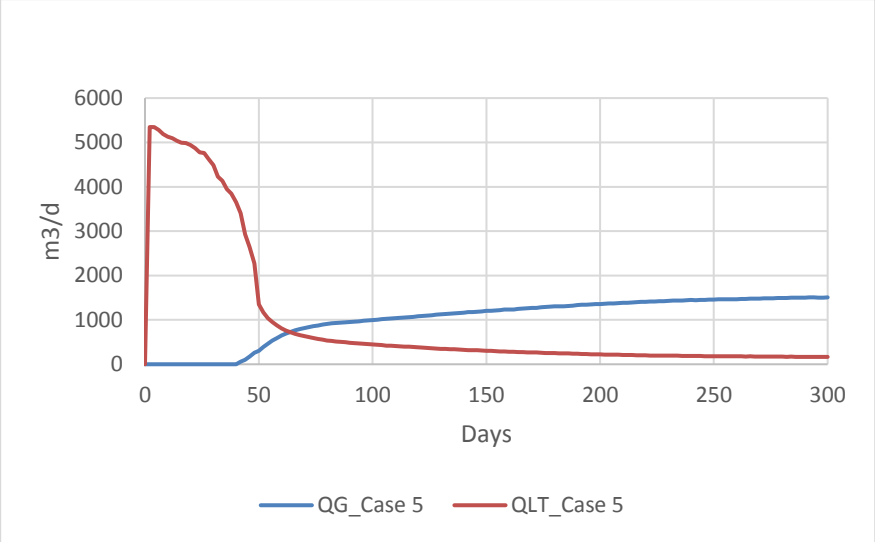


Figure B-4 Gas breakthrough for Case 5

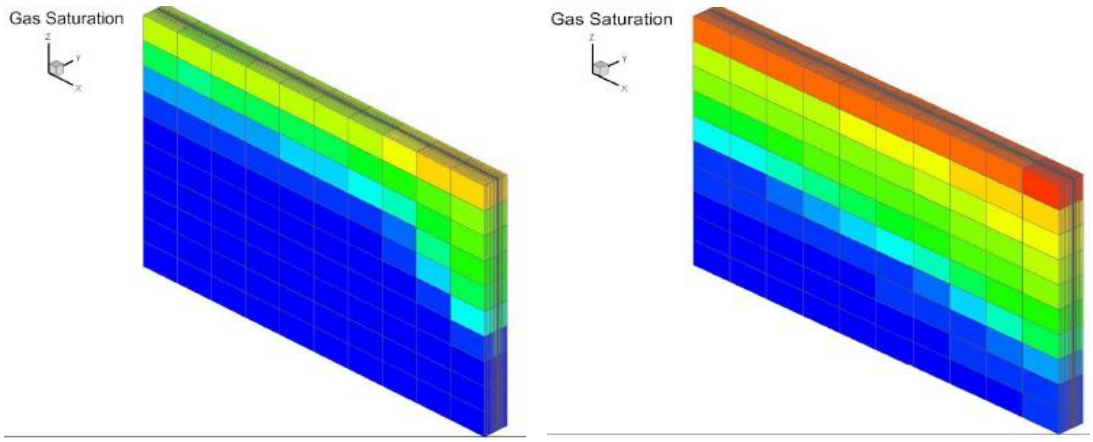


Gas saturation at breakthrough after 42$^{th}$ day  Gas saturation at 300$^{th}$ day

Figure B-5 Gas distribution for case 1

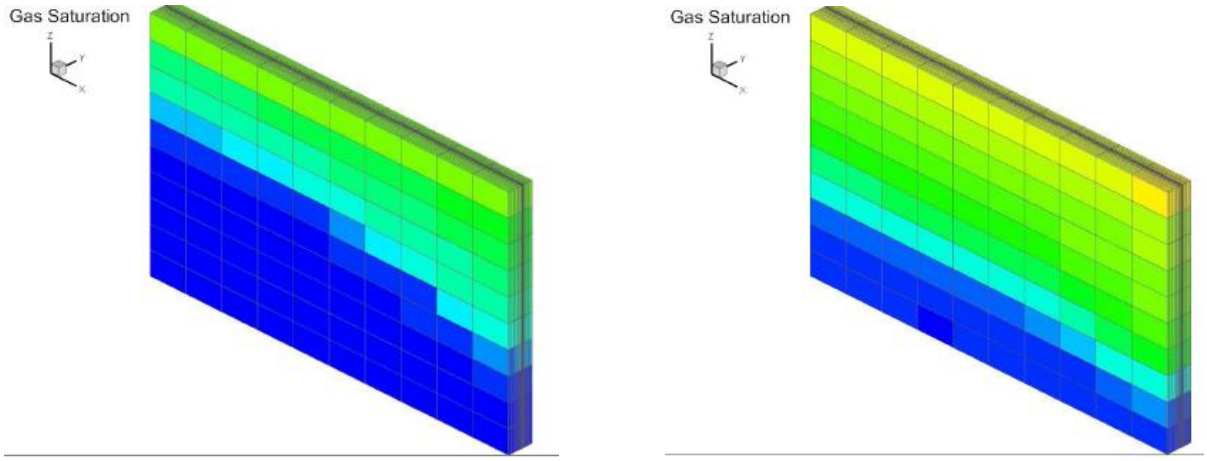


Gas saturation at gas breakthrough  Gas saturation after 300 days

Figure B-6 Gas distribution for case 4

Table B-1 Relative Permeability data used in ROCX-model [18]

| Sw | Krw | Krg |
|---|---|---|
| 0 | 0 | 0 |
| 0.22 | 0 | 0 |
| 0.25 | 1.02E-11 | 0.00040509 |
| 0.3 | 2.62E-08 | 0.0032407 |
| 0.35 | 1.27E-06 | 0.010938 |
| 0.4 | 1.72E-05 | 0.025926 |
| 0.45 | 0.0001223 | 0.050637 |
| 0.5 | 0.00059002 | 0.0875 |
| 0.55 | 0.0021964 | 0.13895 |
| 0.6 | 0.0067901 | 0.20741 |
| 0.65 | 0.018254 | 0.29531 |
| 0.7 | 0.044008 | 0.40509 |
| 0.75 | 0.097233 | 0.53918 |
| 0.8 | 0.2 | 0.7 |
| 1 | 1 | 1 |

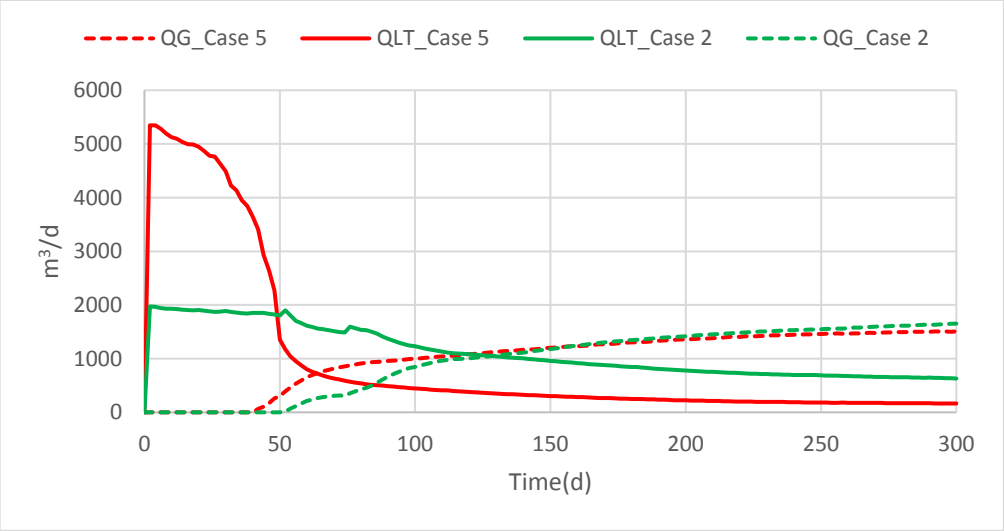


Figure B-7 Gas breakthrough for Case 2 and Case 5

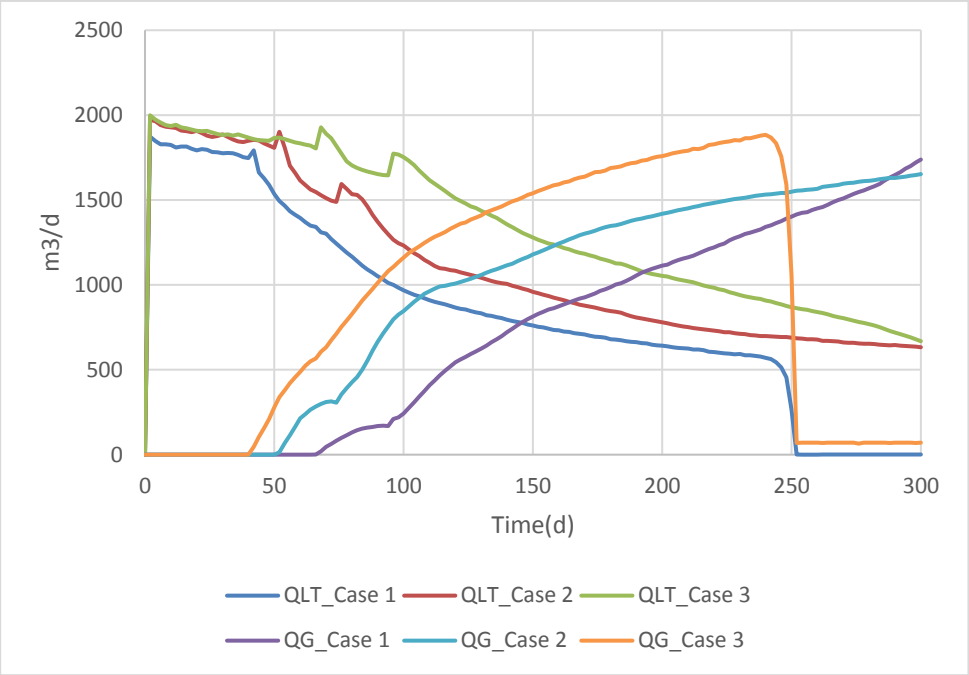


Figure B-8 Gas breakthrough for ICD valves

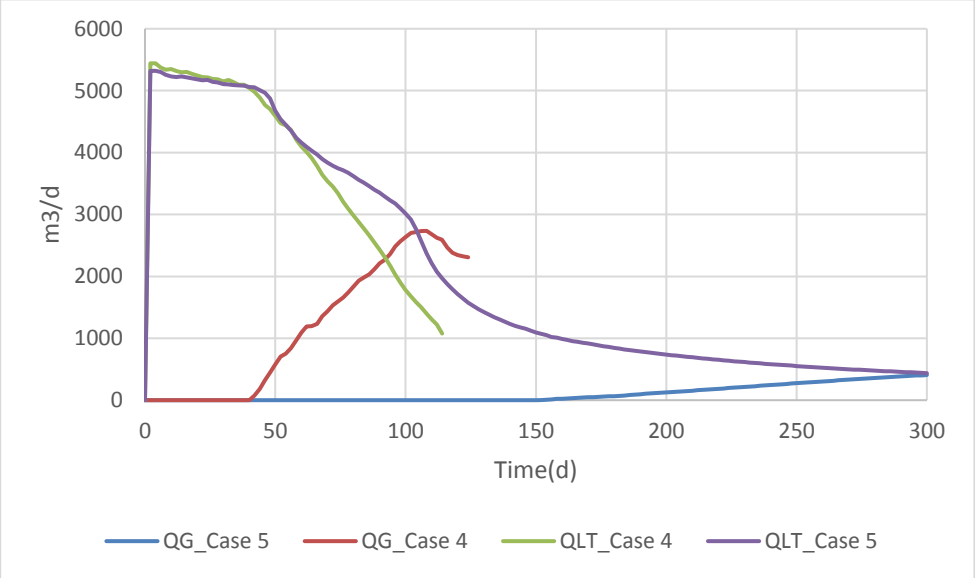


Figure B-9 Gas breakthrough for AICV valves

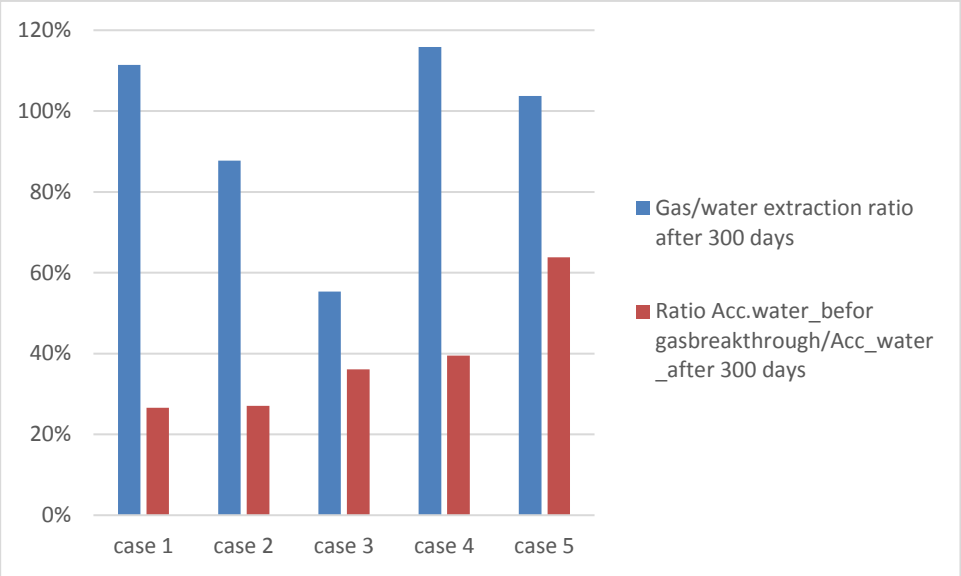


Figure B-10 Effectivity in water extraction and gas bi-production (Low ratio gas/water and high ratio water/water productions–high efficient)

# |Appendix C

**Calculation of CO2 storage capacity in modeled reservoir**

Using equation [3-3] from Chapter 3.2 and assumption for an average storage coefficient value of 0.35, the storage capacity in the simulated volume is:

- *Area of simulated reservoir: a = 1000 m·66 m = 66 000 $m^2$*
- *Capacity of storage of the reservoir model with a storage efficiency of 35%:*
  *Q = 66 000 $m^2$ · 50 m · 0.7 · 0.35 · 274.76 kg/$m^3$ · 0.35 = 0.223 Mt $CO_2$* *[C-1]*

At reservoir conditions of 100 °C and 130 bar:

$$\rho_{CO2} = 274.76 \ \frac{\mathrm{kg}}{\mathrm{m^3}} \qquad [C\text{-}2]$$

$$\rho_{water} = 964.29 \ \frac{\mathrm{kg}}{\mathrm{m^3}} \qquad [C\text{-}3]$$

$$\rho = \frac{\mathrm{m}}{\mathrm{V}} \qquad [C\text{-}4]$$

$$m = \rho \cdot V \qquad [C\text{-}5]$$

$$V_{extracted\ water} = V_{replaced\ with\ CO2} \qquad [C\text{-}6]$$

$$V_{extracted\ fluid} = V_{extracted\ CO2} + V_{extracted\ water} \qquad [C\text{-}7]$$

*Storage efficiency of the model = Total possible $CO_2$ amount to store at reservoir conditions after 300 days(or before gas breakthrough)(Mt) / Capacity of storage of the model* *[C-8]*

Table C-1 $CO_2$ storage efficiency in the modeled ROCX-volume

| Case | Approximately total amount of extracted fluid after 300 days(Mt) | Total amount of extracted water after 300 days(Mt) | Total possible $CO_2$ amount to store at reservoir conditions after 300 days (Mt) | Total possible $CO_2$ amount to store at reservoir before gas breakthrough(Mt) | $CO_2$ storage efficiency in the simulated volume after 300 days | $CO_2$ storage efficiency in the simulated volume before gas breakthrough |
|---|---|---|---|---|---|---|
| Case 1 | 0.27 | 0.12 | 0.035 | 0.010 | 15% | 4.5% |
| Case 2 | 0.32 | 0.16 | 0.046 | 0.011 | 21% | 5% |
| Case 3 | 0.32 | 0.19 | 0.055 | 0.011 | 25% | 5% |
| Case 4 | 0.52 | 0.23 | 0.066 | 0.030 | 30% | 13.5% |
| Case 5 | 0.31 | 0.14 | 0.041 | 0.027 | 19% | 12% |

# Appendix D:

**Cost calculations**

### Costs of compression and reinjection of $CO_2$

*Total costs of $CO_2$ storage = 80 USD/t $CO_2$ · Total amount of extracted $CO_2$ in each case – Total possible $CO_2$ amount to store at reservoir conditions · $CO_2$ revenues* *[D-1]*

$$\frac{p_{res} \cdot V_{res}}{T_{res}} = \frac{p_{surf} \cdot V_{surf}}{T_{surf}} \qquad [D\text{-}2]$$

At standard conditions of 15 °C and 1 atm:

$$\rho_{CO2} = 1.8475 \ \frac{\text{kg}}{\text{m}^3}$$

$$m_{CO2} = \rho_{CO2} \cdot V_{CO2} \qquad [D\text{-}3]$$

Costs after 300 days of gas accumulations:

Case 1

From *[D-2]*: $V_{CO2}$ = 14 272 556 $m^3$

From *[D-3]*: $m_{CO2}$=26.4 Mt $CO_2$

From *[D-1]*: Total cost = 26.4· $10^6$ t $CO_2$· *80 USD/t $CO_2$* -0.035· $10^6$t $CO2$ · *55 USD/t $CO_2$* ≈ *2.1 billion* USD

Case 2

From *[D-2]*: $V_{CO2}$ = 14 749 897 $m^3$

From *[D-3]*: $m_{CO2}$=27.25 Mt $CO_2$

From *[D-1]*: Total cost = 27.25· $10^6$ t $CO_2$· *80 USD/t $CO_2$* -0.046$t$ $CO2$ · $10^6$ · *55 USD/t $CO_2$* ≈ *2.2 billion* USD

Case 3

From *[D-2]*: $V_{CO2}$ = 11 179 525 $m^3$

From *[D-3]*: $m_{CO2}$=20.7 Mt $CO_2$

From *[D-1]*: Total cost = 20.7· $10^6$ t $CO_2$· *80 USD/t $CO_2$* -0.055$t$ $CO2$ · $10^6$ · *55 USD/t $CO_2$* ≈ *1.65 billion* USD

Case 4

From *[D-2]*: $V_{CO2}$ = 27 916 287 $m^3$

From *[D-3]*: $m_{CO2}$=51.6 Mt $CO_2$

From *[D-1]*: Total cost

51.6· $10^6$ t $CO_2$· *80 USD/t* $CO_2$ -0.066· $10^6$t CO2 · *55 USD/t* $CO_2$ ≈ *4.2 billion* USD

Case 5

From *[D-2]*: $V_{CO2}$ = 15 431 125 $m^3$

From *[D-3]*: $m_{CO2}$=28.65 Mt $CO_2$

From *[D-1]*: Total cost

28.65· $10^6$ t $CO_2$· *80 USD/t* $CO_2$ -0.041· $10^6$CO2 · *55 USD/t* $CO_2$ ≈ *2.3 billion* USD

Storage $CO_2$ revenues if no gas breakthrough (assuming average breakthrough time to about 50 days):

From, Table *[C-1]*, expressions *[C-6], [D-3]* and a revenue price/t $CO_2$ at 55USD/t $CO_2$:

Case 1: about 0.55 *mill USD*

Case 2: about 0.605 *mill USD*

Case 3: about 0.605 *mill* USD

Case 4: about 1.65 *mill USD*

Case 5: about 1.5 *mill USD*